LMSC-HEC TR F268584-II

FINAL REPORT

SPACE SHUTTLE MAIN ENGINE STRUCTURAL ANALYSIS AND DATA REDUCTION/EVALUATION

VOLUME 2: HIGH PRESSURE OXIDIZER TURBO-PUMP TURBINE END BEARING ANALYSIS

April 1989

Contract NAS8-37282

Prepared for

NATIONAL AERONAUTICS AND SPACE ADMINISTRATION
GEORGE C. MARSHALL SPACE FLIGHT CENTER, AL 35812

by

Gregory A. Sisk

Lockheed
Missiles & Space Company, Inc.
Huntsville Engineering Center
4800 Bradford Blvd., Huntsville, AL 35807

FINAL REPORT

SPACE SHUTTLE MAIN ENGINE STRUCTURAL ANALYSIS AND DATA REDUCTION/EVALUATION

VOLUME 2: HIGH PRESSURE OXIDIZER TURBO-PUMP TURBINE END BEARING ANALYSIS

April 1989

Contract NAS8-37282

Prepared for

NATIONAL AERONAUTICS AND SPACE ADMINISTRATION
GEORGE C. MARSHALL SPACE FLIGHT CENTER, AL 35812

by
Gregory A. Sisk

Lockheed
Missiles & Space Company, Inc.
Huntsville Engineering Center
4800 Bradford Blvd., Huntsville, AL 35807

FOREWORD

This volume of the final report summarizes the analysis performed on the high pressure oxidizer turbo-pump (HPOTP) turbine end bearing assembly located on the Space Shuttle Main Engine. The static stress analysis was performed by Gregory A. Sisk in the Structures & Mechanics Section of the Lockheed-Huntsville Engineering Center under Contract NAS8-37282.

TABLE OF CONTENTS

LIST OF TABLES

LIST OF FIGURES

LIST OF FIGURES (Continued)

LIST OF FIGURES (Continued)

1. INTRODUCTION

The high-pressure oxidizer turbo-pump (HPOTP) consists of two centrifugal pumps, on a common shaft, that are directly driven by a hot-gas turbine. Pump shaft axial thrust is balanced in that the double-entry main inducer/impeller is inherently balanced and the thrusts of the preburner pump and turbine are nearly equal but opposite. Residual shaft thrust is controlled by a self-compensating, non-rubbing, balance piston. Shaft hang-up must be avoided if the balance piston is to perform properly. One potential cause of shaft hang-up is contact between the Phase II bearing support and axial spring cartridge of the HPOTP main pump housing. This analysis investigates the status of the bearing support/axial spring cartridge interface under current loading conditions.

An ANSYS version 4.3, three-dimensional, finite element model was generated on Lockheed's VAX 11/785 computer. A nonlinear thermal analysis was then executed on the Marshall Space Flight Center Engineering Analysis Data System (EADS). These thermal results were then applied along with the interference fit and bolt preloads to the model as load conditions for a static analysis to determine the gap status of the bearing support/axial spring cartridge interface.

For possible further analysis of local regions of the HPOTP main pump housing assembly, detailed ANSYS submodels have been generated using I-DEAS Geomod and Supertab (Appendix A).

2. MODEL DESCRIPTION

The following tables identify components and element types of the HPOTP Turbine End Bearing assembly and provide current values of the number of nodes and elements for the ANSYS finite element model of each component. Table 1 provides this information for a heat transfer thermal analysis and Table 2 gives it for a structural static analysis. The user should note that the bolt and radial gap elements are null for the thermal analysis while the convection link elements are null for the static analysis. A complete description of the element types, including KEYOPT parameters, for both the thermal and static analyses is given in Tables 3 and 4, respectively.

Table 1 HPOTP TURBINE END BEARING THERMAL ANALYSIS NODES, ELEMENTS, AND ELEMENT TYPES FOR COMPONENTS

Component	Drawing No.	Nodes	Elements	Element Types
Pump Housing	RS007729-151	3644	2555	1
Bearing Support	RS007975-003	900	468	2
Axial Spring Cartridge	RS007974-013	2064	778	3
Anti-Vortex Ring	RS007973-003	2250	1152	4
Retainer Ring	RS007920-007	2448	1476	5
Spacer	RS007784-173	324	144	6
Bolts (18)	RS007945-003			0
Convection Links			864	8 through 15
Radial Gaps				0
TOTALS		11630	7437	

Table 2 HPOTP TURBINE END BEARING STATIC ANALYSIS NODES, ELEMENTS, AND ELEMENT TYPES FOR COMPONENTS

Component	Drawing No.	Nodes	Elements	Element Types
Pump Housing	RS007729-151	3644	2555	1
Bearing Support	RS007975-003	900	468	2
Axial Spring Cartridge	RS007974-013	2064	778	3
Anti-Vortex Ring	RS007973-003	2250	1152	4
Retainer Ring	RS007920-007	2448	1476	5
Spacer	RS007784-173	324	144	6
Bolts (18)	RS007945-003	180	162	7
Convection Links				0
Radial Gaps			720	16 through 18
TOTALS		11810	7455	

Table 3 HPOTP MAIN PUMP HOUSING ASSEMBLY MODEL ELEMENT TYPES FOR THERMAL ANALYSIS

No.	Type	KEYOPT										Description
1	70	0	0	0	0	0	0	0	0	0	0	ISOPAR. SOLID, THERMAL
2	70	0	0	0	0	0	0	0	0	0	0	ISOPAR. SOLID, THERMAL
3	70	0	0	0	0	0	0	0	0	0	0	ISOPAR. SOLID, THERMAL
4	70	0	0	0	0	0	0	0	0	0	0	ISOPAR. SOLID, THERMAL
5	70	0	0	0	0	0	0	0	0	0	0	ISOPAR. SOLID, THERMAL
6	70	0	0	0	0	0	0	0	0	0	0	ISOPAR. SOLID, THERMAL
7	0											NULL
8	34	0	0	0	0	0	0	0	0	0	0	CONVECTION LINK
9	34	0	0	0	0	0	0	0	0	0	0	CONVECTION LINK
10	34	0	0	0	0	0	0	0	0	0	0	CONVECTION LINK
11	34	0	0	0	0	0	0	0	0	0	0	CONVECTION LINK
12	34	0	0	0	0	0	0	0	0	0	0	CONVECTION LINK
13	34	0	0	0	0	0	0	0	0	0	0	CONVECTION LINK
14	34	0	0	0	0	0	0	0	0	0	0	CONVECTION LINK
15	34	0	0	0	0	0	0	0	0	0	0	CONVECTION LINK
16	0											NULL
17	0											NULL
18	0											NULL

Table 4 HPOTP MAIN PUMP HOUSING ASSEMBLY MODEL ELEMENT TYPES FOR STATIC ANALYSIS

No.	Type	KEYOPT										Description
1	45	0	0	0	0	0	0	0	0	0	0	ISOPAR. STRESS SOLID, 3-D
2	45	0	0	0	0	0	0	0	0	0	0	ISOPAR. STRESS SOLID, 3-D
3	45	0	0	0	0	0	0	0	0	0	0	ISOPAR. STRESS SOLID, 3-D
4	45	0	0	0	0	0	0	0	0	0	0	ISOPAR. STRESS SOLID, 3-D
5	45	0	0	0	0	0	0	0	0	0	0	ISOPAR. STRESS SOLID, 3-D
6	45	0	0	0	0	0	0	0	0	0	0	ISOPAR. STRESS SOLID, 3-D
7	4	0	0	0	0	0	0	0	0	0	0	ELASTIC BEAM, 3-D
8	0											NULL
9	0											NULL
10	0											NULL
11	0											NULL
12	0											NULL
13	0											NULL
14	0											NULL
15	0											NULL
16	52	0	0	0	0	0	0	0	0	0	0	INTERFACE ELEM. 3-D
17	52	0	0	0	0	0	0	0	0	0	0	INTERFACE ELEM. 3-D
18	52	0	0	0	0	0	0	0	0	0	0	INTERFACE ELEM. 3-D

A single ANSYS FILE16 has been created which contains all of the elements given in Tables 1 and 2. The user can select which analysis file (FILE27) to write by issuing one of several sets of ANSYS commands. For a thermal analysis, the following commands are used.

COMMAND	COMMENT
/prep7	enter PREP7 routine
resume	
/title,THERMAL	ANALYSIS
nall	select all nodes
eall	select all elements
kan,-1	set analysis type to thermal
et,7,0	null bolt elements
et,8,34	convection link elements
rp8,1,0	
et,16,0	null radial gap elements
rp3,1,0	
afwrit	analysis file write
/eof	exit PREP7 routine

For a static analysis, the following commands are issued.

COMMAND	COMMENT
/prep7	enter PREP7 routine
resume	
/title,STATIC	ANALYSIS
nall	select all nodes
eall	select all elements
kan,0	set analysis type to static
et,7,4	bolt elements
et,8,0	null convection link elements
rp8,1,0	
et,16,52	radial gap elements
rp3,1,0	
afwrit	analysis file write
/eof	exit PREP7 routine

Using different element type numbers for each major component provides a convenient way to select a single component or group of components. For example, to select all the pump housing elements and the nodes associated with these elements, the user can issue the following ANSYS commands.

COMMAND	COMMENT
esel,type,1,1	select pump housing elements
nelem	select pump housing nodes

For all of the Phase II bearing components, the following commands apply.

COMMAND	COMMENT
esel,type,2,7	select Phase II bearing component elements
nelem	select Phase II bearing component nodes

These commands can be issued in either the PREP7 or POST1 routines.

For a thermal analysis, Table 5 identifies the convection link elements used for the HPOTP turbine end bearing interfaces. In addition, the number of elements, material constant numbers, element type numbers and real constant numbers is given for each interface. These elements correspond to the contact and gap conductances given in Section 4, Thermal Environment.

Table 5 HPOTP MAIN PUMP HOUSING ASSEMBLY MODEL CONVECTION LINK ELEMENTS

Interface	Elements	Material	Type	Real
Pump Housing/ Bearing Support	288	8 and 9	8 and 9	8 through 11
Pump Housing/ Axial Spring Cartridge	72	10	10	12
Pump Housing/ Anti-Vortex Ring	72	11	11	13
Pump Housing/ Retainer Ring	72	12	12	14
Pump Housing/ Spacer	144	13	133	15 and 16
Bearing Support/ Axial Spring Cartridge	72	14	14	17
Axial Spring Cartridge/ Anti Vortex Ring	144	15	15	18 and 19
TOTAL	864			

For a static analysis, Table 6 identifies the radial gap and interference elements used for the HPOTP turbine end bearing interfaces. In addition, the number of elements, element type numbers, and real constant numbers is given for each interface. Nominal radii for interference fits have been adjusted to provide the correct orientation of STIF52 elements. All interference fit and gap elements use an interface stiffness of 20 x 10^6 lbf/in.

Table 6 HPOTP MAIN PUMP HOUSING ASSEMBLY MODEL RADIAL GAP AND INTERFERENCE FITS

Interface (In)	Nominal Radius (In)	Clearance	Elements Real	Type/
Pump Housing/ Bearing Support	3.3430 3.3490	-0.0060	72	16 20
Pump Housing/ Axial Spring Cartridge	3.3430 3.3350	0.0080	72	16 21
Pump Housing/ Anti-Vortex Ring	3.3430 3.3350	0.0080	72	16 21
Pump Housing/ Retainer Ring	3.3430 3.3485	-0.0055	72	16 22
Pump Housing/ Spacer	3.3430 3.3410	0.0020	108	16 23
Bearing Support/ Axial Spring Cartridge	2.4080 2.4066	0.0014	144	17 24
Bearing Support/ Axial Spiring Cartridge	2.7865 2.7875	-0.0010	72	17 25
Axial Spring Cartridge/ Anti-Vortex Ring	2.5875 2.5880	-0.0005	108	18 26
Axial Spring Cartridge/ Outer Bearing Race	2.0326 2.0300	0.0026		
TOTAL			720	

Note: Clearance sign follows the ANSYS STIF52 convention, i.e., positive indicates a gap opening and negative indicates interference.

A COSMIC NASTRAN model of the HPOTP Turbine End Bearing pump housing from a previous analysis* was used as a base. It contains the Phase I bearing support and axial spring cartridge. Components of the model are shown in Figure 1 for Section AA of the primary turbine drain system. This section identification follows the nomenclature established in the reference. NASTRAN grid points and coordinate systems were translated to ANSYS using the AUX15 (Input File Translator) routine. CIHEX1 and CWEDGE elements were converted to equivalent STIF45 elements using a FORTRAN 77

*W.H. Armstrong et al. "Stress and Fatigue Analyses of the Space Shuttle Main Engine - Final Report," Contract NAS8-32703, LMSC-HEC TR D784035, December 1980, pp. 9.1-20 program. Each of the 36 sections was plotted individually and compared with the reference to ensure that the translation was accurate and complete.

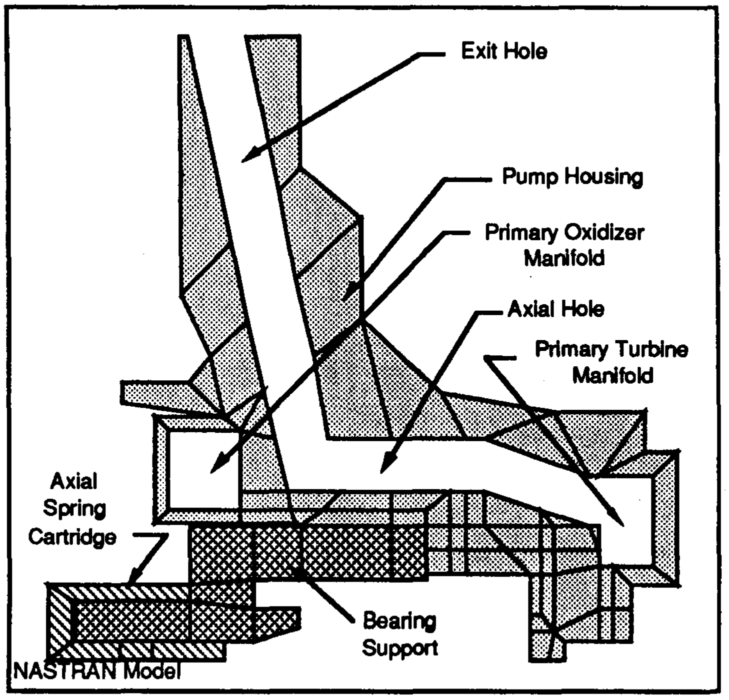

Figure 1 Components of the NASTRAN Main Pump Housing Model with Phase I Bearing Support and Axial Spring Cartridge

We removed the Phase I bearing support and axial spring cartridge, which are identified in Figure 1, from the converted NASTRAN model. The ANSYS pump housing model was then revised to interface with the Phase II bearing support/cartridge components. The modified region is identified in Figure 2. Interface nodes were added and positioned to match those of the Phase II bearing support/cartridge models.

All the Phase II bearing component models were developed under this contract. The bearing support, axial spring cartridge, anti-vortex ring, retainer ring, and spacer models are identified in Figure 3. Nodes have been positioned between all component interfaces and the pump housing interface to provide the correct alignment for the convection link and radial gap elements given in Tables 3 and 4, respectively.

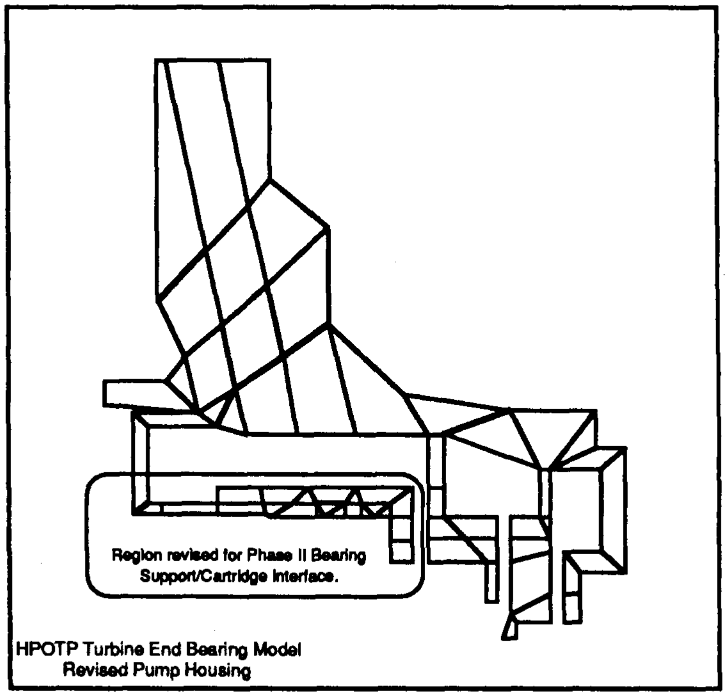

Figure 2 HPOTP Main Pump Housing Model (Region Modified for Phase II Bearing Support/Cartridge Interface)

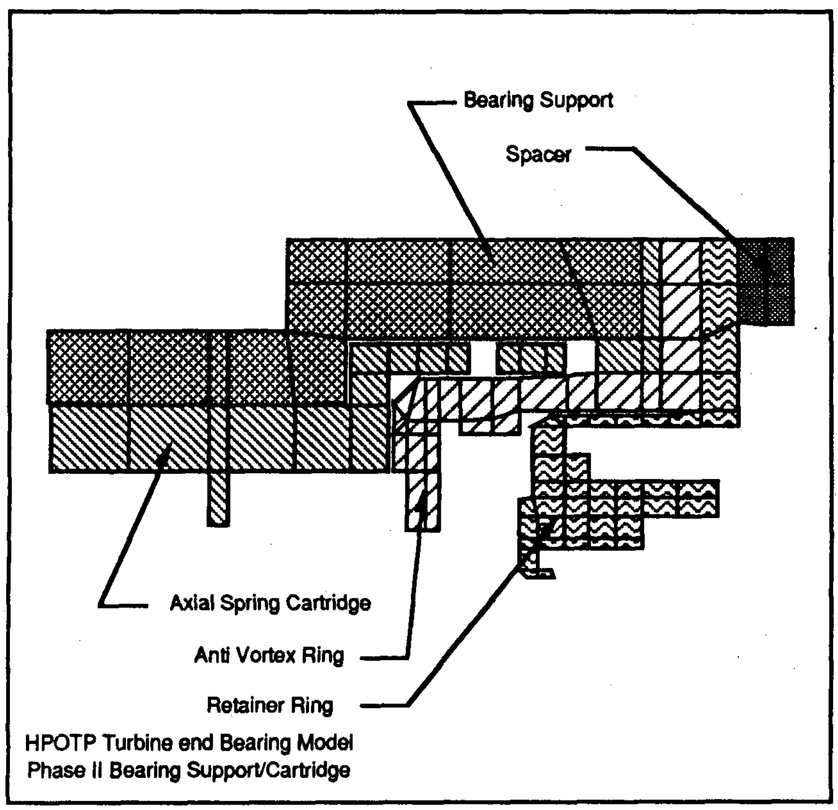

Figure 3 Components of the Phase II Bearing Support/Cartridge Model

The element sums listed in Table 2 include axial contact elements between Phase II bearing components. However, these elements were removed from the model and replaced with coupled degree-of-freedom sets. The rationale for this decision is that the components will remain in axial contact due to the bolt preload. An example of a typical bolt interface with the Phase II bearing support, axial spring cartridge, anti-vortex ring, retainer ring, and spacer components is shown in Figure 4. The bolt is coupled in the axial translational direction at only one point on the bearing support, which represents the bolt head. The remaining bolt/component interfaces model the shank portion of the bolt.

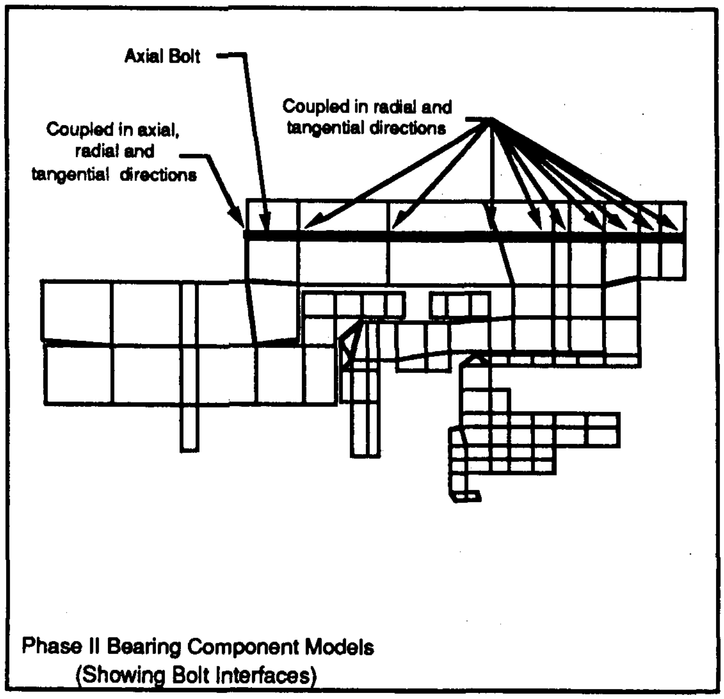

Figure 4 Coupled Degrees of Freedom for Bolt Interfaces of Phase II Bearing Support/Cartridge Models

The ANSYS integrated system model, including bearing support bolt, convection link, and radial gap elements, for the HPOTP Turbine End Bearing analysis is shown in Figure 5. This model represents the analysis tool for subsequent thermal and structural analysis to determine interference at the bearing support/axial spring cartridge interface.

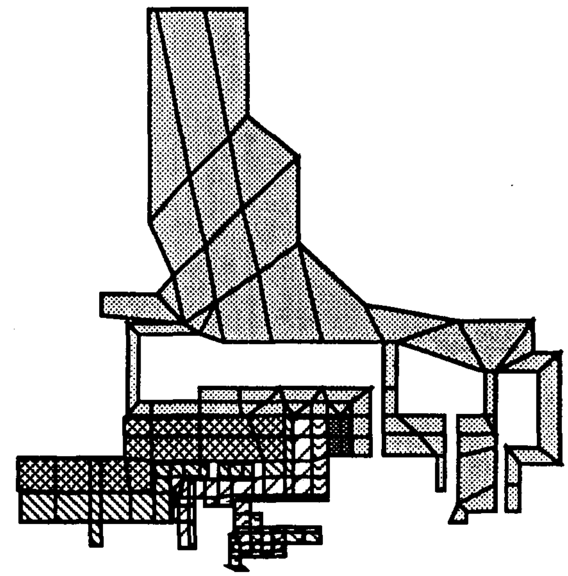

Figure 5 ANSYS Integrated System Model for the HPOTP Turbine End Bearing Analysis

For the presentation of thermal and static analyses results, section locations of the pump housing drain system exit holes are identified in Figure 6. Sections AA and CC (Θ = 26 and 146°) represent the primary turbine drain exit holes. The Sections DD (Θ = 86 and 166°) represent the secondary turbine drain and Sections BB and NN (Θ = -14, -74 and -114°) represent the primary oxidizer drain.

The gap elements along the bearing support/axial spring cartridge interface are identified in Figure 7. The status (open or closed) of these gap elements under the combined loading of bolt preload, interference fits and thermal stress yields the final results of this analysis.

An extensive library of ANSYS command data blocks has been assembled into an ANSYS User File (FILE35). Some of these data blocks were used to build the finite element model, modify it, apply boundary conditions and loads, and construct the plots presented within this document. A few of these ANSYS command data blocks and the plots which they produced are presented in Figures 8 through 15 as an illustration. These

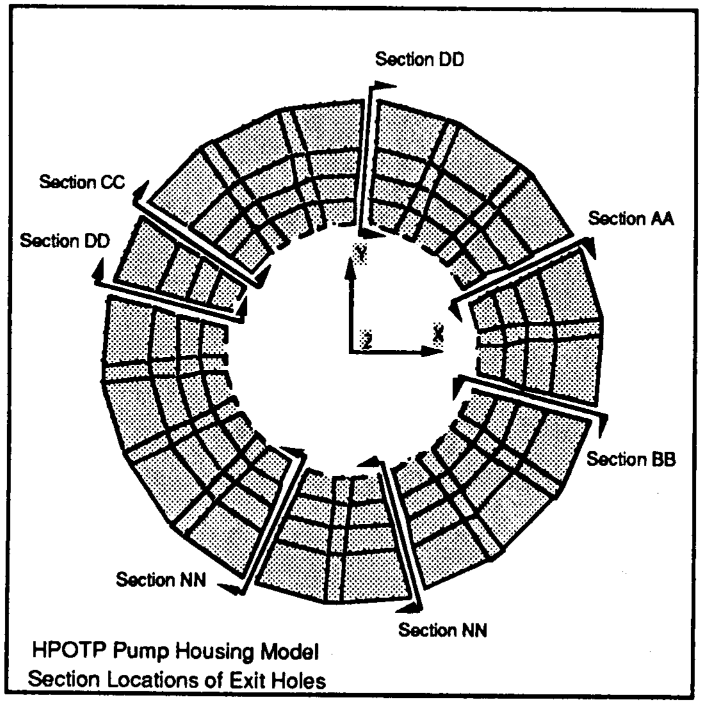

Figure 6 Drain System Section Locations for the HTOTP Turbine End Bearing Analysis

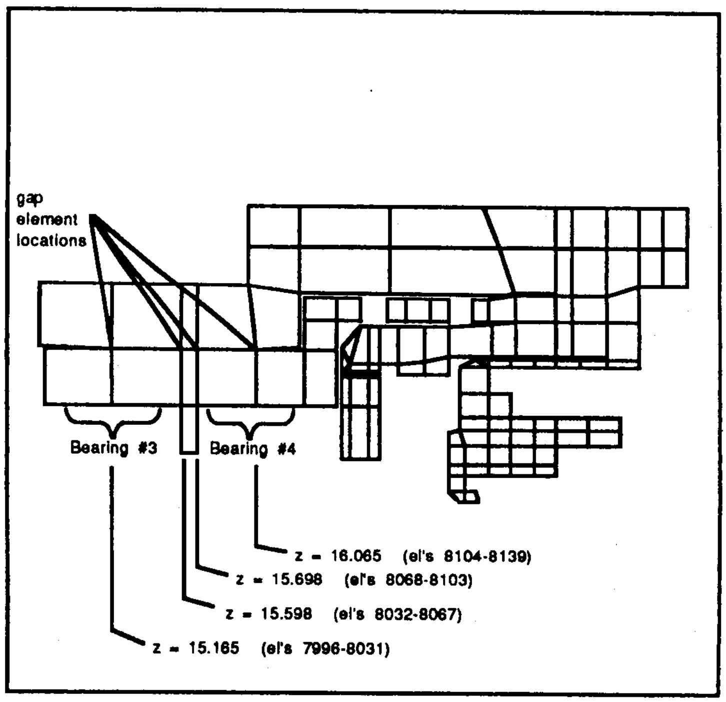

Figure 7 Gap Element Locations Along the Bearing Support/ Axial Spring Cartridge Interface

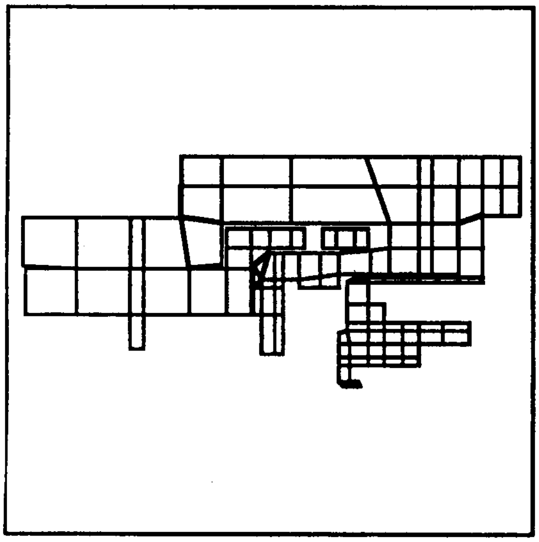

ANSYS USER FILE

```
astart
nsel,node,4001,13500
csys,1
nrse,y,0,2
enod,0
csys,0
/show,4207,,1
dsys,0
   psi    =    (atan(1.)/45.)
   xvrf   =    -sin(psi)
   yvrf   =    cos(psi)
/view,1,xvrf,yvrf,0
/title,SUPPORT/CARTRIDGE CROSS
        SECTION
/pnum,defa
/num,-1
/pbc,defa
/type,1,0
/zoom,1,off
eplo
/eof
```

Figure 8 ANSYS User File (ASTART) for Element Plot of HPOTP Phase II Bearing Support/Cartridge Models

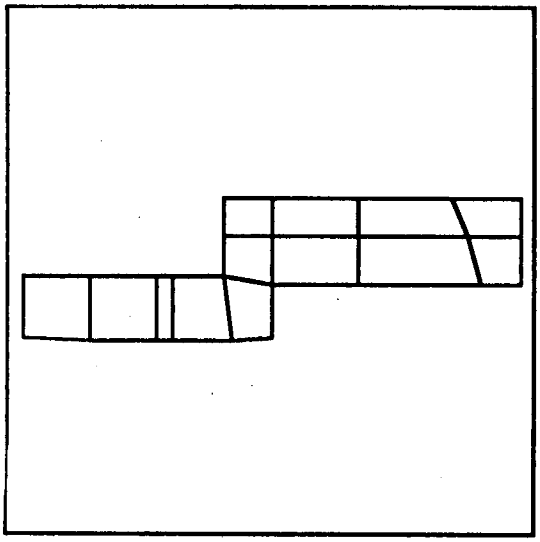

```
ANSYS USER FILE
bstart
nsel,node,4001,5000
csys,1
nrse,y,0,2
enod,0
csys,0
/show,4207,,1
dsys,0
   psi      =      (atan(1.)/45.)
   xvrf        =        -sin(psi)
   yvrf        =         cos(psi)
/view,1,xvrf,yvrf,0
/title,SUPPORT  CROSS  SECTION
/pnum,defa
/num,-1
/pbc,defa
/type,1,0
/zoom,1,off
eplo
/eof
```

Figure 9 ANSYS User File (BSTART) for Element Plot of HPOTP Phase II Bearing Support Model

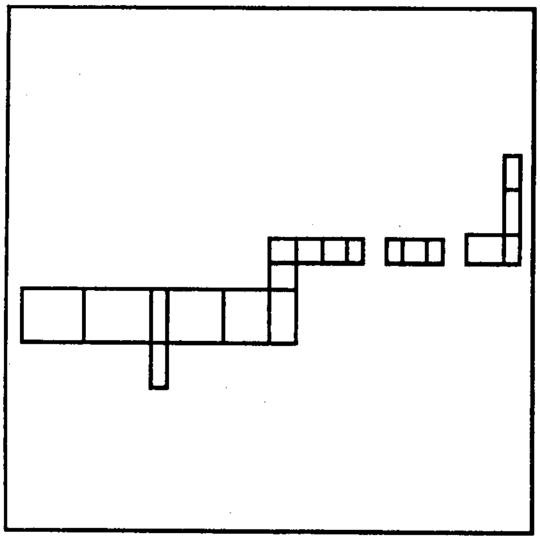

ANSYS USER FILE

```
cstart
nsel,node,5001,7500
csys,1
nrse,y,0,2
enod,0
csys,0
/show,4207,,1
dsys,0
   psi     =     (atan(1.)/45.)
   xvrf    =          -sin(psi)
   yvrf    =           cos(psi)
/view,1,xvrf,yvrf,0
/title,AXIAL SPRING CARTRIDGE CROSS
        SECTION
/pnum,defa
/num,-1
/pbc,defa
/type,1,0
/zoom,1,off
eplo
/eof
```

Figure 10 ANSYS User File (CSTART) for Element Plot of HPOTP Phase II Axial Spring Cartridge Model

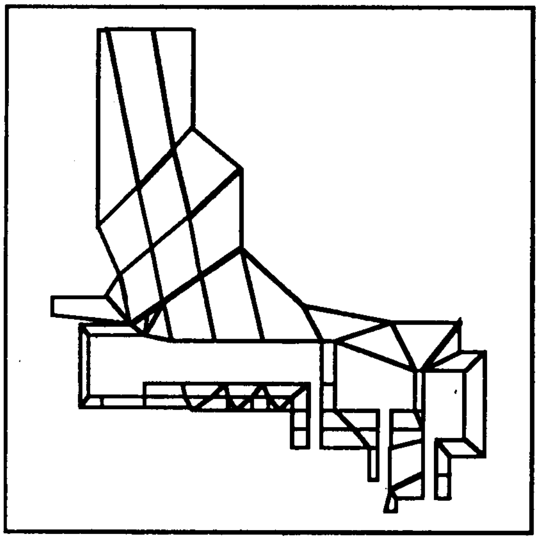

```
ANSYS USER FILE
hstart
csys,1
cscir,1,0
nsel,node,1,4000
nrse,y,-4,16
enod,1
nrse,y,-4,6
csys,0
/show,4207,,1
dsys,0
   psi    =    (atan(1.)/45.)
   xvrf   =    -sin(psi)
   yvrf   =    cos(psi)
/view,1,xvrf,yvrf,0
/title,PUMP HOUSING CROSS SECTION
/pnum,defa
/num,-1
/pbc,defa
/type,1,0
/zoom,1,off
eplo
/eof
```

Figure 11 ANSYS User File (HSTART) for Element Plot of HPOTP Main Pump Housing Model

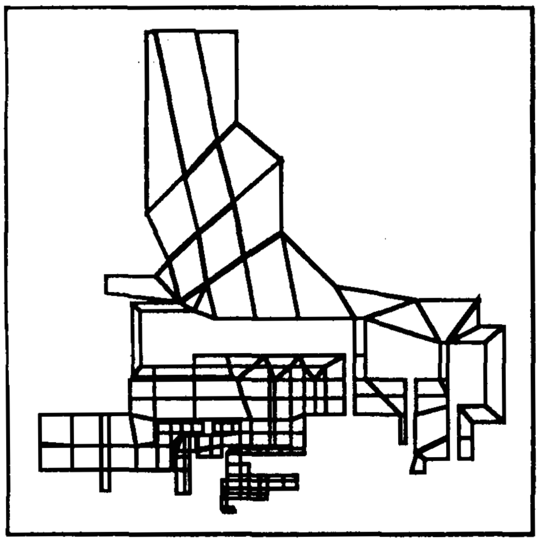

```
ANSYS USER FILE
nstart
csys,1              $cscir,1,0
nrse,y,-4,16
enod,1
nrse,node,4001,13500  $nrse,y,0,2
nase,node,1,4000      $nrse,y,-4,6
csys,0
/show,4207,,1
dsys,0
   rpd     =     (atan(1.)/45.)
   psi     =           rpd*6.
   xvrf    =        -sin(psi)
   yvrf    =         cos(psi)
/view,1,xvrf,yvrf,0
/title,TURBINE END BEARING CROSS
         SECTION
/pnum,defa
/num,-1
/pbc,defa
/type,1,0
/zoom,1,off
eplo
/eof
```

Figure 12 ANSYS User File (NSTART) for Element Plot of HPOTP Main Pump Housing Assembly Model

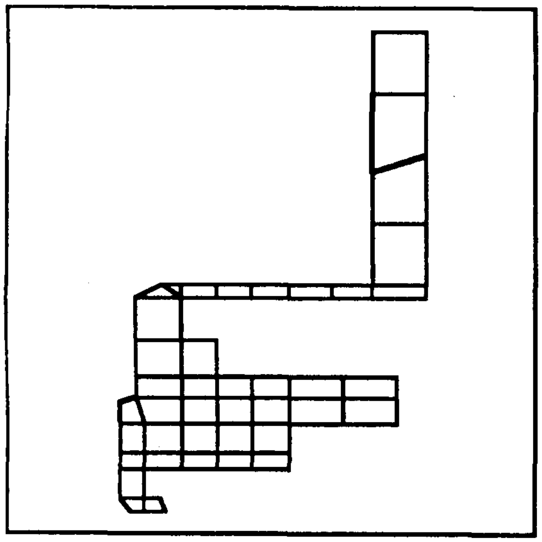

ANSYS USER FILE
rstart
nsel,node,10001,12500
csys,1
nrse,y,0,2
enod,0
csys,0
/show,4207,,1
dsys,0
psi = (atan(1.)/45.)
xvrf = -sin(psi)
yvrf = cos(psi)
/view,1,xvrf,yvrf,0
/title,RETAINER RING CROSS SECTION
/pnum,defa
/num,-1
/pbc,defa
/type,1,0
/zoom,1,off
eplo
/eof

Figure 13 ANSYS User File (RSTART) for Element Plot of HPOTP Phase II Retainer Ring Model

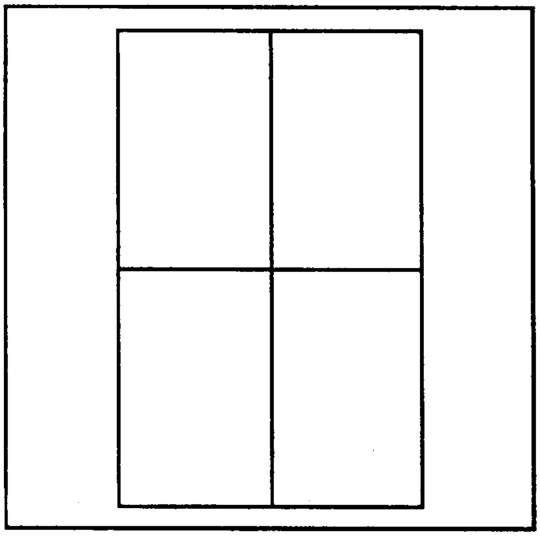

ANSYS USER FILE

```
sstart
nsel,node,13001,13500
csys,1
nrse,y,0,2
enod,0
csys,0
/show,4207,,1
dsys,0
   psi    =    (atan(1.)/45.)
   xvrf   =        -sin(psi)
   yvrf   =         cos(psi)
/view,1,xvrf,yvrf,0
/title,SPACER CROSS SECTION
/pnum,defa
/num,-1
/pbc,defa
/type,1,0
/zoom,1,off
eplo
/eof
```

Figure 14 ANSYS User File (SSTART) for Element Plot of HPOTP Phase II Spacer Model

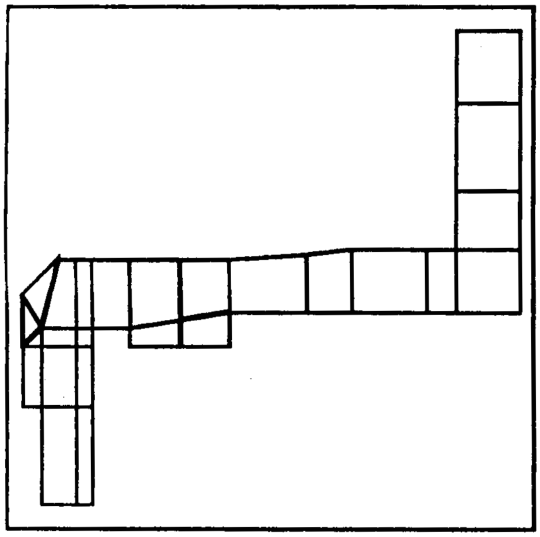

ANSYS USER FILE

```
vstart
nsel,node,7501,10000
csys,1
nrse,y,0,2
enod,0
csys,0
/show,4207,,1
dsys,0
    psi    =    (atan(1.)/45.)
    xvrf   =    -sin(psi)
    yvrf   =    cos(psi)
/view,1,xvrf,yvrf,0
/title,ANTI VORTEX RING CROSS
          SECTION
/pnum,defa
/num,-1
/pbc,defa
/type,1,0
/zoom,1,off
eplo
/eof
```

Figure 15 ANSYS User File (VSTART) for Element Plot of HPOTP Phase II Anti-Vortex Ring Model data blocks produce cross-sectional views of the finite element models at their node start position. As an example, the HSTART data block in Figure 11 is executed by issuing the following ANSYS commands.

COMMAND	COMMENT
*ufile,house,auf	set user file to HOUSE.AUF
*use,hstart	plot cross-sectional view of pump housing model at node start section

In addition, node numbers for a user selected region may be displayed by supplying the following subsequent commands.

COMMAND	COMMENT
/zoom,1	zoom to a user selected region
/pnum,node,1	turn on node numbering
/num,2	
eplo	produce element plot

A cutaway view of the ANSYS three-dimensional finite element model of the HPOTP pump housing is shown in the hidden line plot of Figure 16. This view and all remaining plots in this section are from the turbine end towards the pump end. A 90° section (from $\Theta = -24°$ to 66°) has been removed from the models to show their internal structure. Cutaway views of the bearing support and axial spring cartridge models are presented in Figures 17 and 18, respectively. Cutaway views of the anti-vortex ring, retainer ring, and spacer are presented in Figures 19, 20, and 21, respectively.

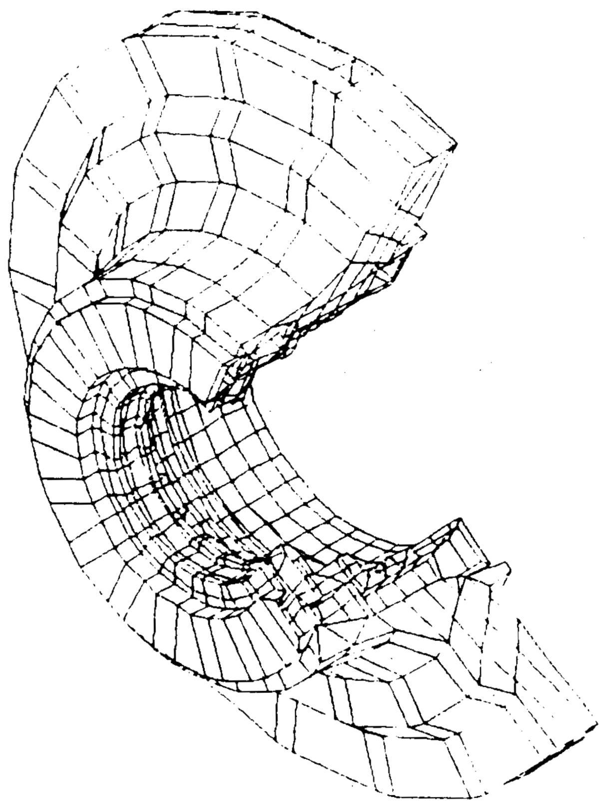

Figure 16 HPOTP Main Pump Housing Model (Cutaway View from Turbine End toward Pump)

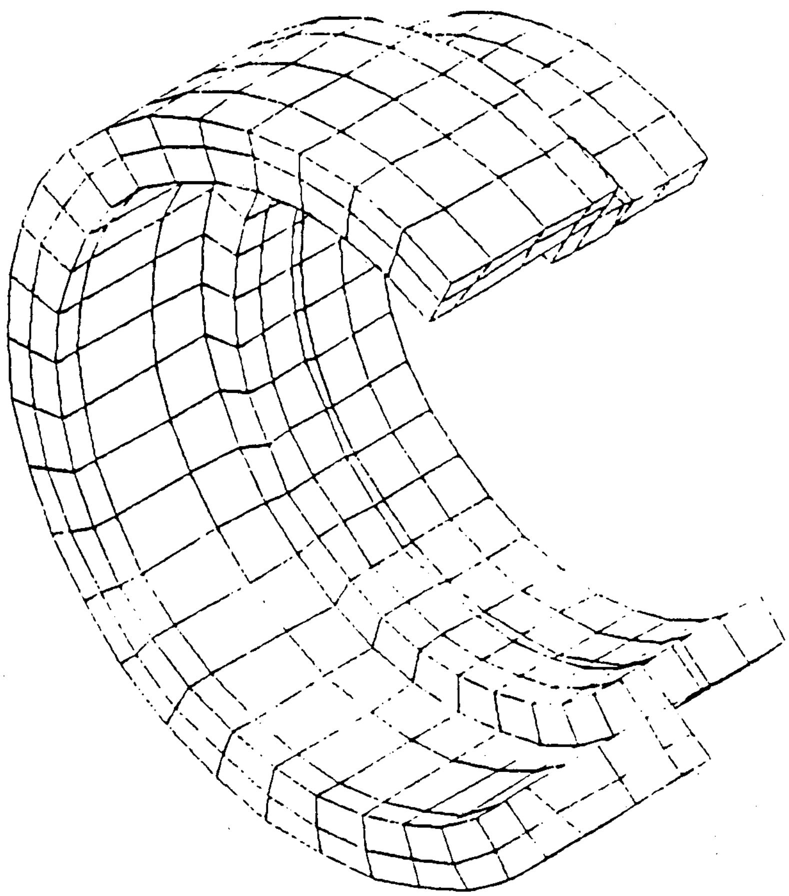

Figure 17 HPOTP Phase II Bearing Support Model (Cutaway View from Turbine End toward Pump)

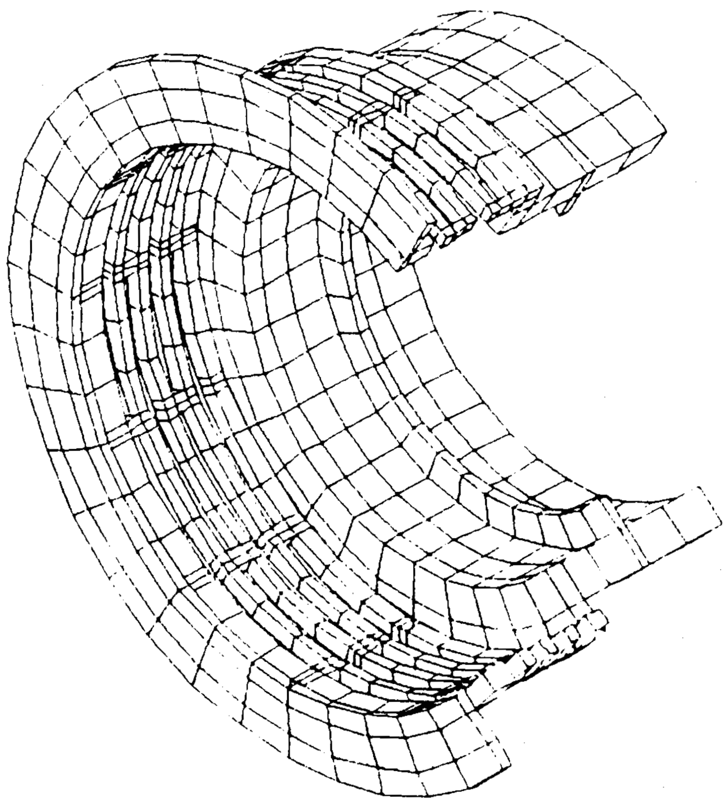

Figure 18 HPOTP Phase II Axial Spring Cartridge Model
(Cutaway View from Turbine End toward Pump)

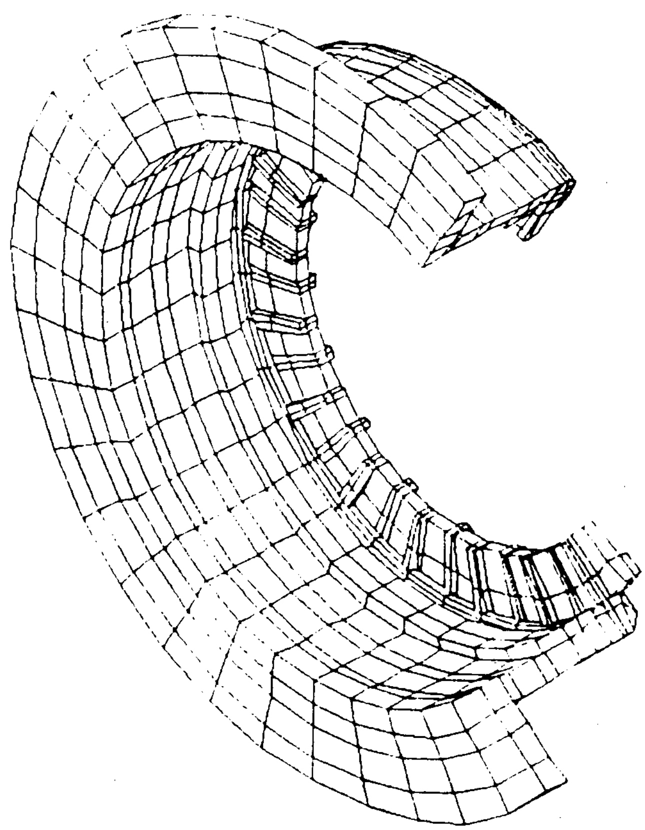

Figure 19 HPOTP Phase II Anti-Vortex Ring Model
(Cutaway View from Turbine End toward Pump)

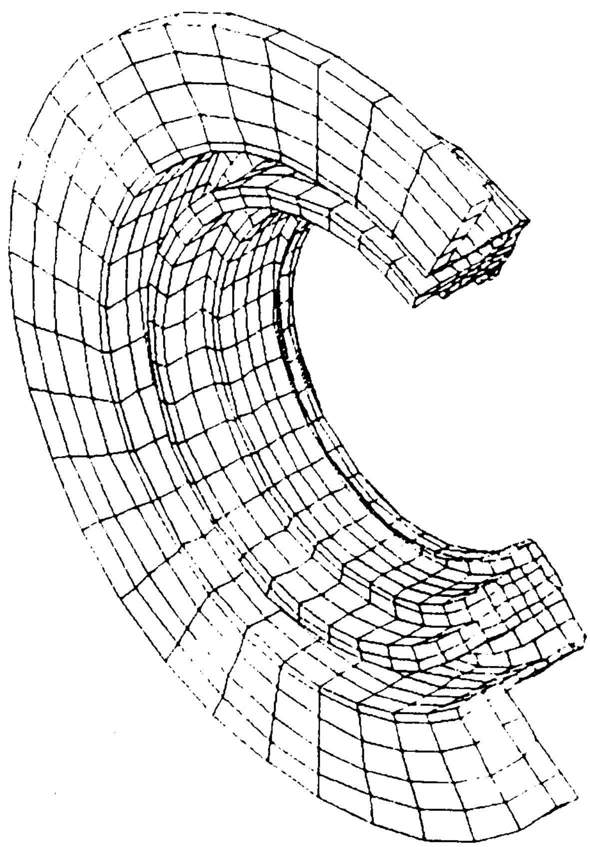

Figure 20 HPOTP Phase II Retainer Ring Model
(Cutaway View from Turbine End toward Pump)

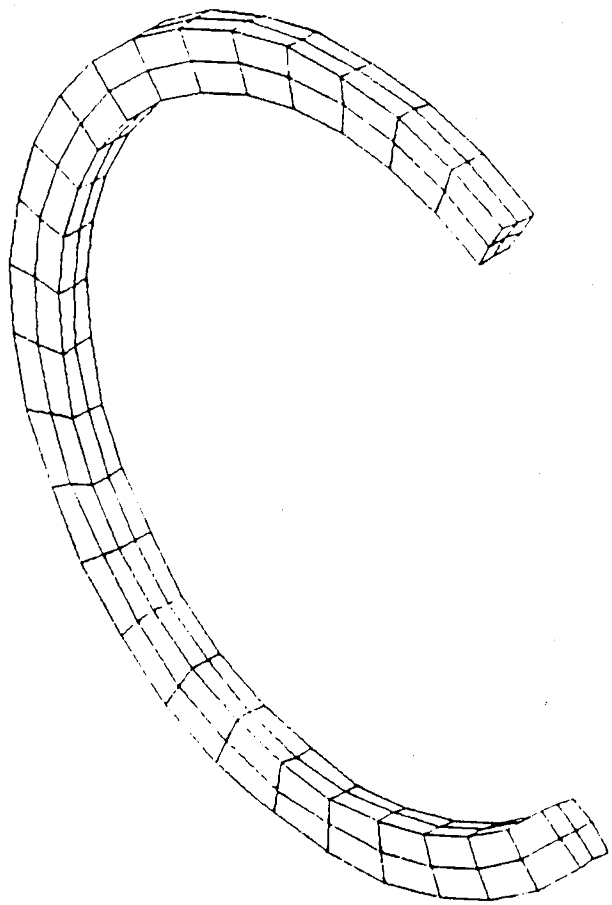

Figure 21 HPOTP Phase II Spacer Model (Cutaway View from Turbine End toward Pump)

3. MATERIAL PROPERTIES

The materials used in the HPOTP Turbine End Bearing components are given in Table 7. In addition, we have identified the reference for obtaining their thermal and mechanical properties.

Table 7 HPOTP TURBINE END BEARING MATERIALS

COMPONENT	MATERIAL	REFERENCE
Pump Housing	INCONEL 718	Rockwell
Bearing Support	INCONEL 718	Rockwell
Axial Spring Cartridge	INCONEL 718	Rockwell
Anti Vortex Ring	INCONEL 718	Rockwell
Retainer Ring	INCONEL 718	Rockwell
Spacer	INCONEL 718	Rockwell
Bolts (18)	A286 STEEL	Rockwell

INCONEL 718 material property data, obtained from the Rockwell Materials Properties Manual, were curve fitted to cubic polynomials for ANSYS input over the temperature range of 0 to 2000 °R. Extrapolation beyond 2000 °R is questionable. However, the expected temperature range for this analysis is from 100 to 1500 °R, well within the selected curve fit limits. Figure 22 shows the coefficient of thermal conductivity as a function of absolute temperature. Young's modulus, Poisson's ratio,and the coefficient of thermal expansion for INCONEL 718 as functions of absolute temperature are presented in Figures 23, 24 and 25, respectively.

In addition, the following material properties for the A286 steel bolts are used:

Coefficient of Thermal Conductivity (k) = 8.68 Btu/in/°R
Young's Modulus (E) = 29.1×10^6 lbf/in^2
Poisson's Ratio (ν) = 0.29
Coefficient of Thermal Expansion (α) = 0.917×10^{-5} in/in/°R

These are assumed constant over the absolute temperature range from 0 to 2300 °R.

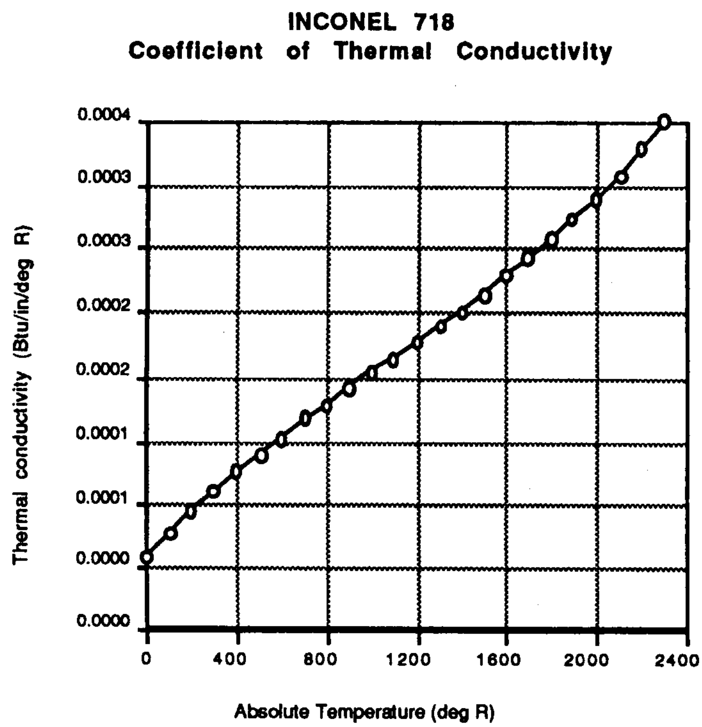

Figure 22 INCONEL 718 Coefficient of Thermal Conductivity as a Function of Absolute Temperature

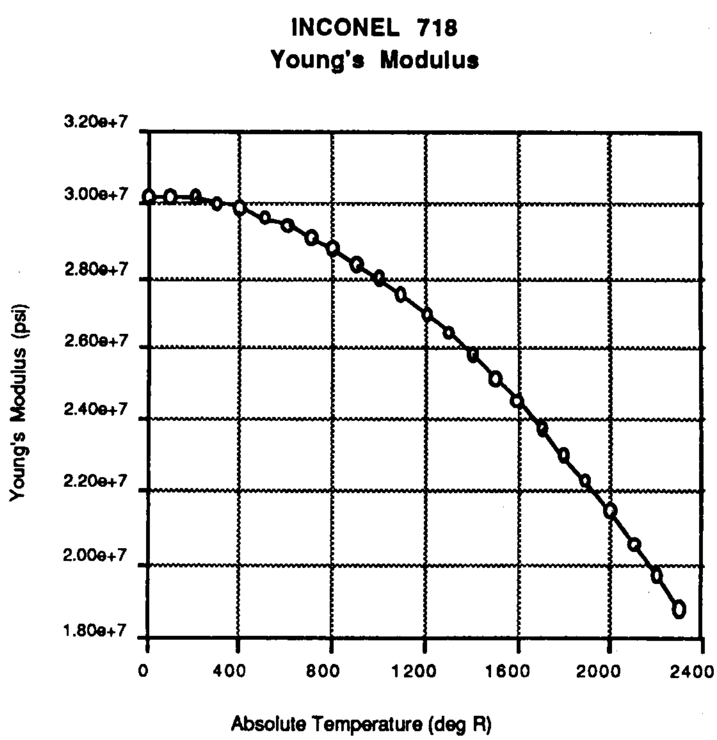

Figure 23 INCONEL 718 Young's Modulus as a Function of Absolute Temperature

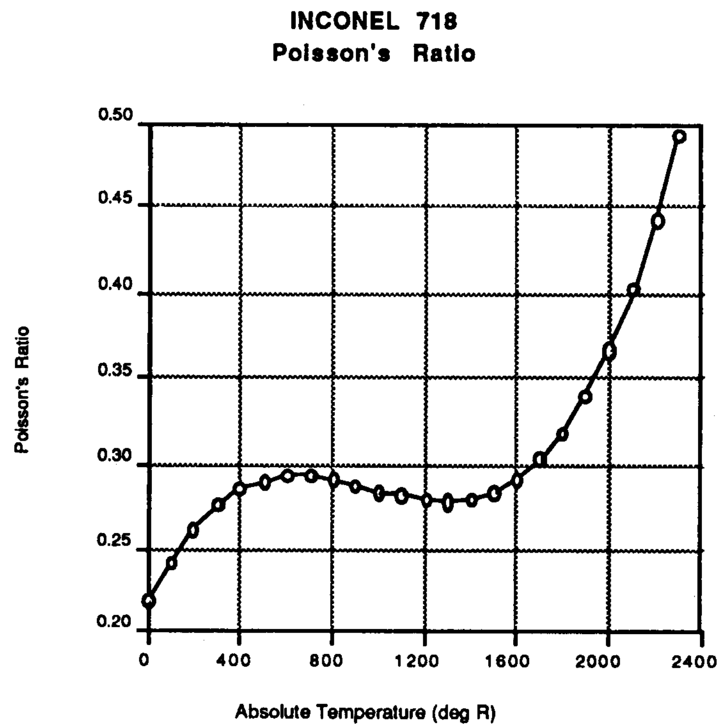

Figure 24 INCONEL 718 Poisson's Ratio as a Function of Absolute Temperature

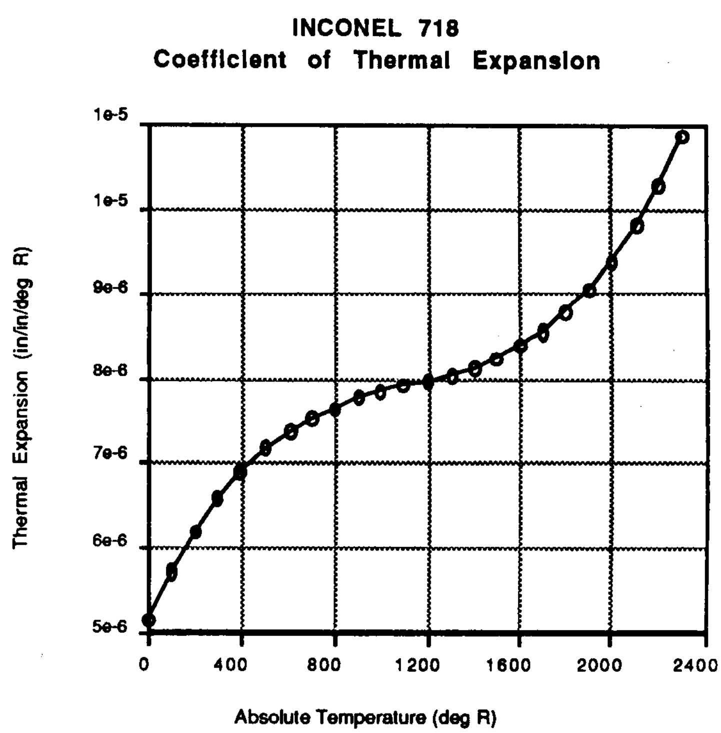

Figure 25 INCONEL 718 Coefficient of Thermal Expansion as a Function of Absolute Temperature

4. THERMAL ENVIRONMENT

Heat transfer coefficients were calculated for the HPOTP pump housing and turbine end bearing using the following empirical equations for pipe flow.

For turbulent flow

$$Nu = 0.023\ Re^{0.8}\ Pr^{0.4}$$

and for laminar flow between the bearing support and axial spring cartridge

$$Nu = 1.86\ (Re\ Pr\ D/L)^{0.33}\ (\mu_b/\mu_s)^{0.14}$$

where

Nu = Average Nusseelt number
Re = Reynolds number
Pr = Prandtl number
D = Hydraulic diameter of passage
L = Length of passage
μ_b = Fluid viscosity at bulk temperature
μ_s = Fluid viscosity at surface temperature.

Computation of the thermal environment for the HPOTP pump housing was performed by Gene Teal, LMSC-HEC, and checked and verified by Glenn Wilmer, EP62, NASA-MSFC Turbomachinery and Combustion Devices Branch. Mr. Wilmer recommended increasing the secondary turbine drain temperature from 720 to 800 °R and increasing the second stage turbine disk aft cavity temperature from 1000 to 1400 °R. These changes are incorporated in the tables that follow. The drain system leakage flow rates and temperatures at steady state Full Power Level (FPL) operation were provided by NASA-MSFC and are given in Table 8.

The locations of radial holes and manifolds for the primary turbine, secondary turbine and primary oxidizer drains are identified in the cross-sectional view of the HPOTP pump housing shown in Figure 26. Circumferential locations of radial holes for the primary turbine, secondary turbine, and primary oxidizer drains are shown in Figures 27 through 29, respectively. Cross-sectional views of the primary turbine, secondary turbine and primary oxidizer drains, showing the drain exit and axial holes, are presented in Figures 30 through 32 for stations $\Theta = 26°$, $86°$, and $-114°$, respectively. Pressures, temperatures, and

Table 8 FLOW RATES AND TEMPERATURES FOR HPOTP MAIN PUMP HOUSING ASSEMBLY SEAL AND DRAIN SYSTEM

SEAL OR DRAIN	FLOW RATE (lbm/s)	TEMPERATURE (°R)
Primary Turbine Seal	0.240	1000
Secondary Turbine Seal	0.016	1000
Primary Oxidizer Seal	0.080	205
Helium Purge	0.046	530
Primary Turbine Drain	0.224	1000
Secondary Turbine Drain	0.039	800
Primary Oxidizer Drain	0.103	400

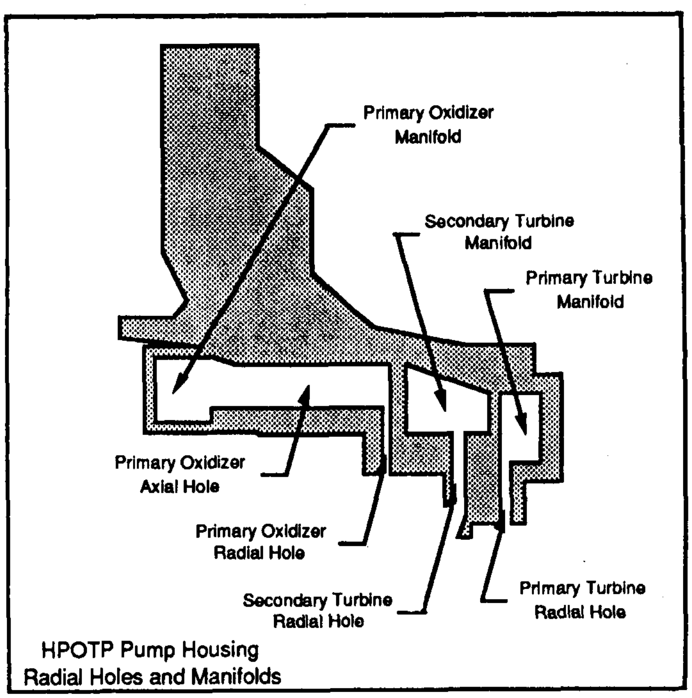

Figure 26 HPOTP Main Pump Housing Radial Holes and Manifolds or Primary Turbine, Secondary Turbine and Primary Oxidizer Drain Systems

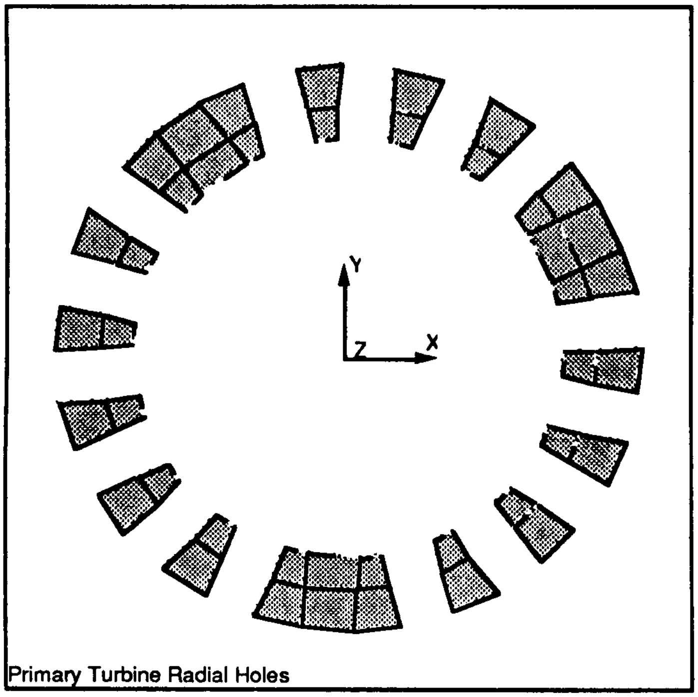

Figure 27 HPOTP Main Pump Housing Radial Holes for Primary Turbine Drain System

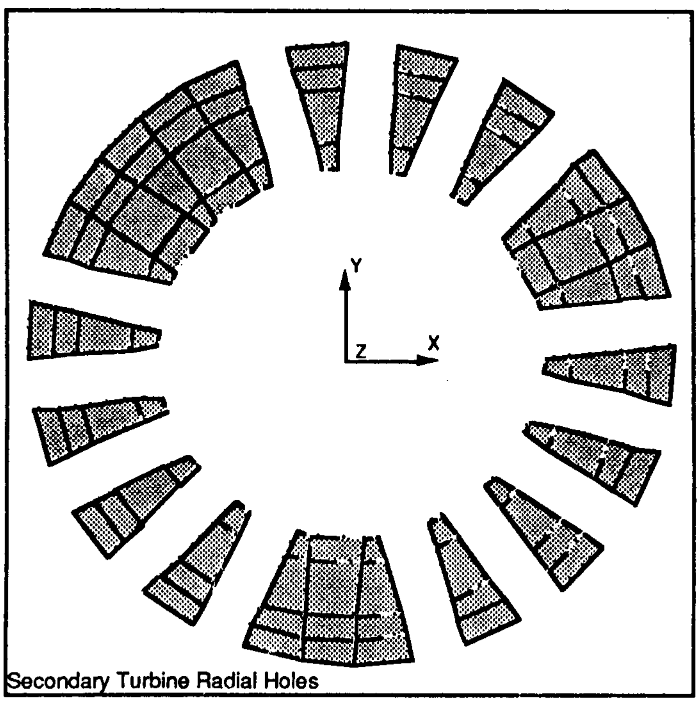

Figure 28 HPOTP Main Pump Housing Radial Holes for Secondary Turbine Drain System

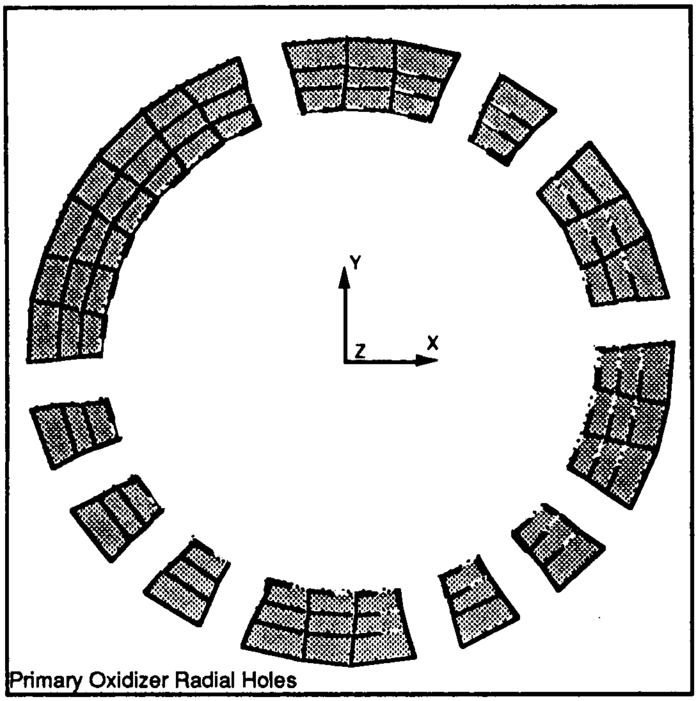

Figure 29 HPOTP Main Pump Housing Radial Holes for Primary Oxidizer Drain System

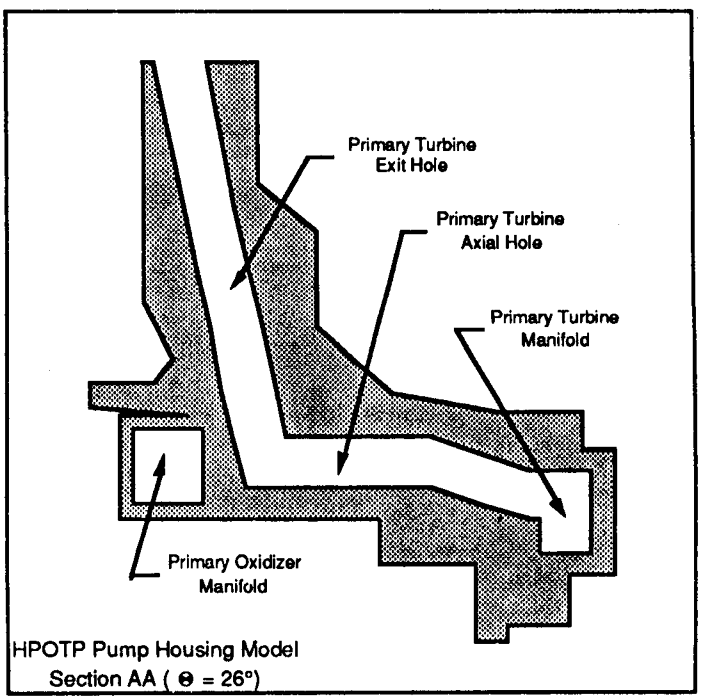

Figure 30 HPOTP Main Pump Housing Exit and Axial Holes for Primary Turbine Drain System (Θ = 26°)

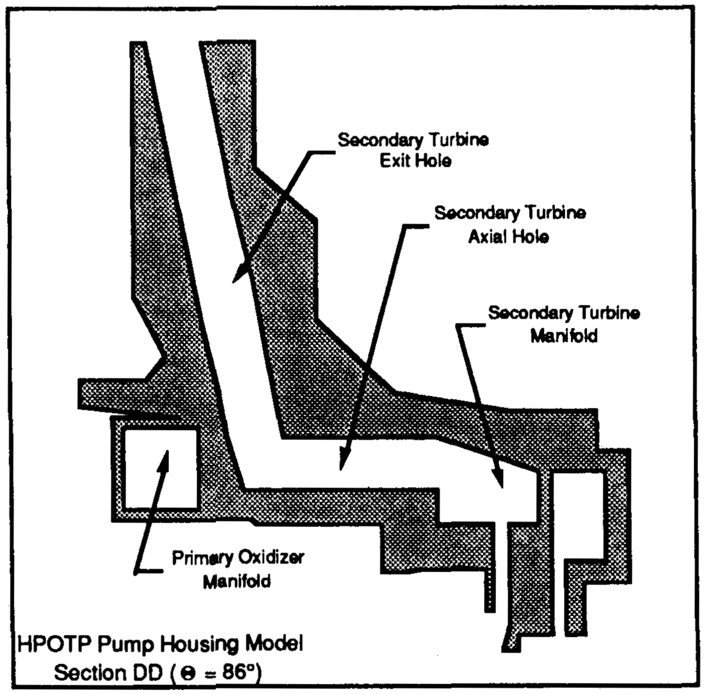

Figure 31 HPOTP Main Pump Housing Exit and Axial Holes for Secondary Turbine Drain System (ϴ = 86°)

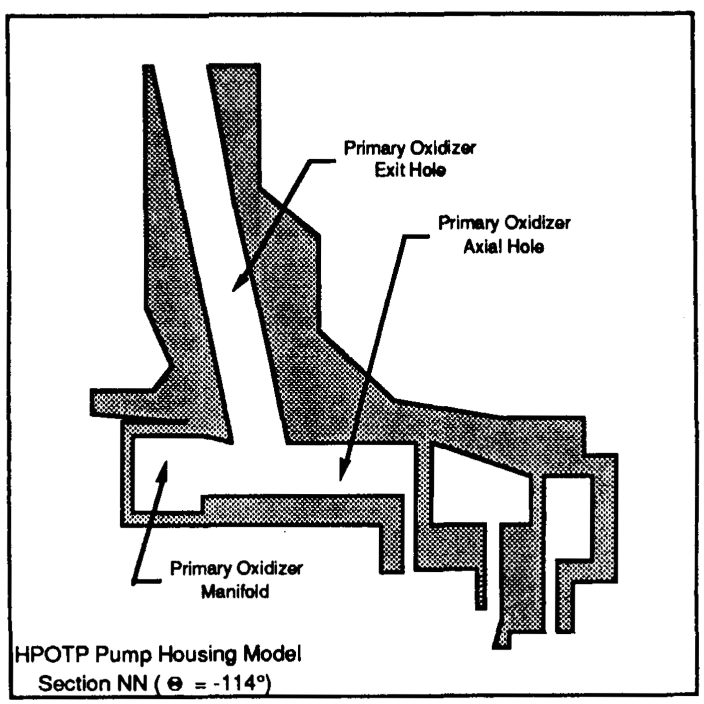

Figure 32 HPOTP Main Pump Housing Exit and Axial Holes for Primary Oxidizer Drain System (ϴ = -114°)

heat transfer coefficients for the primary turbine, secondary turbine, and primary oxidizer drains of the pump housing are given in Table 9.

Heat transfer coefficients were also computed for the mixed coolant manifold, reflector cavity of the turbine discharge strut, and aft cavity of the second stage turbine disk shown in Figure 33. Their thermal environment is presented along with the schematic. Note that the mixed coolant manifold has not been included in the ANSYS finite element model of the pump housing.

The thermal environment of the HPOTP Phase II turbine end bearing components has also been computed. The pressures, temperatures and heat transfer coefficients at the locations shown in Figure 34 for the support and cartridge assembly. The thermal boundary coefficients at bearing locations 1 and 2 are simplifications designed to simulate the outer bearing race to axial spring cartridge heat fluxes. These data were obtained from the analysis performed by Joe Cody of SRS Technologies.

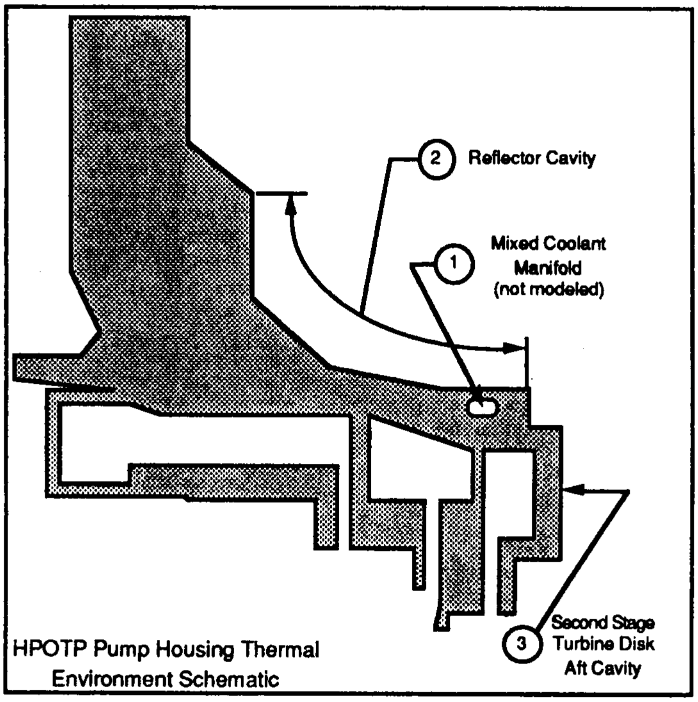

NODE	DESCRIPTION	P (psia)	T (°R)	h_c (Btu/in^2 sec °R)
1	Mixed Coolant Manifold	5000	835	0.0011/0.0053
2	Reflector Cavity	3650	280	0.00113
3	Second Stage Turbine Disk Aft Cavity	3625	1400	0.00034

Figure 33 HPOTP Main Pump Housing Thermal Environment Schematic

Table 9 PRESSURES, TEMPERATURES AND HEAT TRANSFER COEFFICIENTS FOR HPOTP MAIN PUMP HOUSING DRAIN SYSTEM

DRAIN SYSTEM	P (psia)	T (°R)	h_c (Btu/in^2 sec °R)
Primary Turbine Drain:			
15 Radial Holes, 0.261" dia	95	1000	0.0022
Manifold	95	1000	0.00011
1 Exit Hole, 11/16" dia, Θ = 30°	75	1000	0.0017
1 Exit Hole, 11/16" dia Θ = 138°	55	1000	0.0021
Secondary Turbine Drain:			
Inlet Slots	20	800	0.00025
4 Radial Holes, 5/16" dia Θ = 46°-106°	20	800	0.00043
10 Radial Holes, 5/16" dia Θ = 166°-6°	20	800	0.00023
Manifold, Θ = 38°-117°	20	800	0.0001
Manifold, Θ = 146°-16°	20	800	0.00013
1 Exit Hole, 11/16" dia, Θ = 90°	20	800	0.00031
1 Exit Hole, 11/16" dia Θ = 162°	20	800	0.00035
Primary Oxidizer Drain:			
11 Radial Holes, 15/16" dia	20	400	0.00026
3 Axial Holes, 1/2" dia	20	400	0.00012
7 Axial Holes, 39/64" dia	20	400	0.000084
Manifold	20	400	0.000076
3 Axial Holes, 11/16" dia	20	400	0.00018
3 Exit Holes, 11/16" dia	20	400	0.00018

Note: Θ is positive, counterclockwise, looking from the turbine end towards the pump end with the main pump inlet centerline located at Θ = 276°.

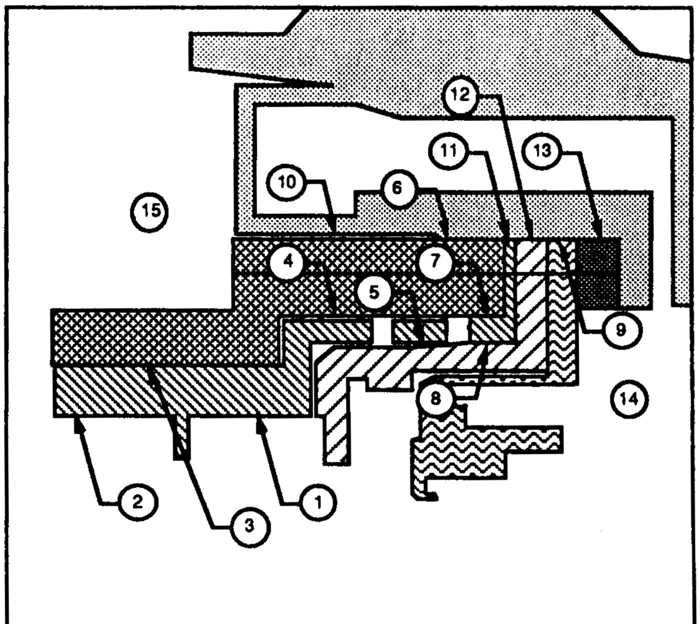

NODE	DESCRIPTION	P (psia)	T (°R)	h_c (Btu/in^2 sec °R)
1	Conductance from Outer Bearing Race to	335	290	0.00014
2	Cartridge	330	350	0.00014
3	Film Coefficient	330	220	0.00084
4	Film Coefficient	335	220	0.00018
5	Film Coefficient	335	220	0.00024
6	Contact Conductance			0.0048
7	Contact Conductance			0.0048
8	Contact Conductance			0.0048
9	Contact Conductance			0.0048
10	Gap Conductance	325		0.000040
11	Gap Conductance	335		0.000019
12	Gap Conductance	335		0.000019
13	Gap Conductance	20		0.000078
14	Film Coefficient	20	400	0.000031
15	Film Coefficient	325	170	0.00092

Figure 34 HPOTP Phase II Bearing Support/Cartridge Thermal Environment Schematic

5. BOUNDARY CONDITIONS AND LOADS

Displacement boundary conditions for the HPOTP pump housing model are shown in Figure 35. The indicated line of nodes is constrained in all three directions around the circumference of the pump housing. No pressure loads were applied to the model for the structural analysis described in Section 7. Therefore, the deformations of the pump housing presented in that section are due strictly to thermal loads.

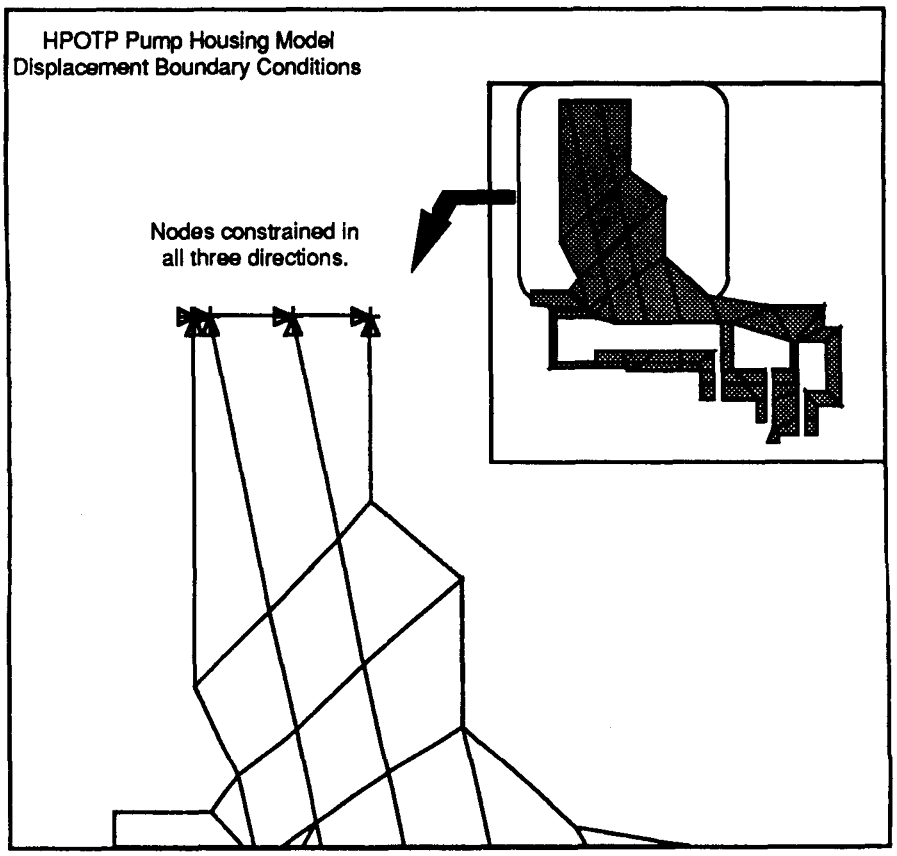

Figure 35 Displacement Boundary Conditions Applied to HPOTP Main Pump Housing Model

For a preliminary static analysis, the preload is 10% of the yield strength in the axial bolts (RS007945-003) which pass through the bearing support, axial spring cartridge, anti-vortex ring, retainer ring and spacer and finally terminate in the pump housing. Figure 36 shows the magnitude, direction, and location of the preload forces imposed on 18 ends of bolt elements imbedded in the spacer. An equal and opposite number of forces are imposed in the corresponding pump housing nodes where the bolts terminate. Hence, the overall system is in static equilibrium.

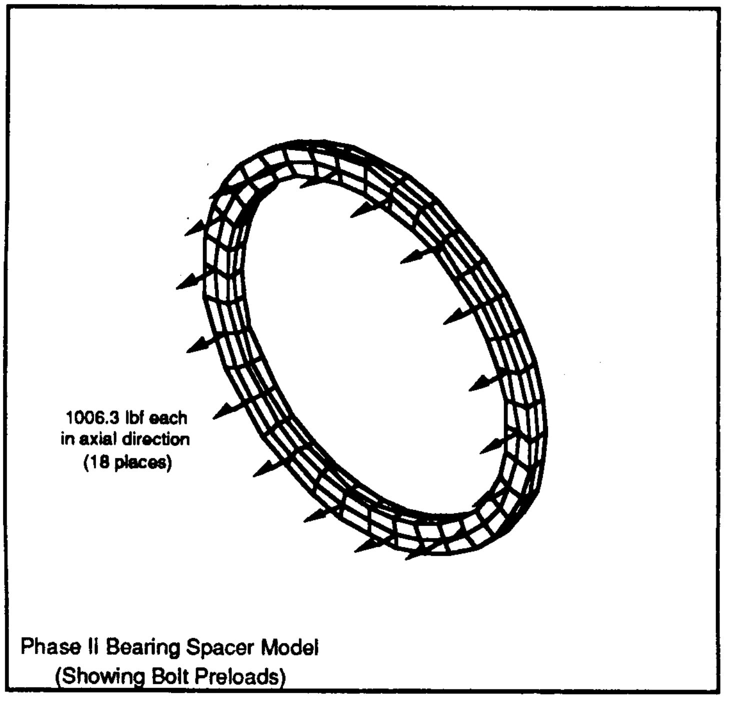

Figure 36 Bolt Preloads Shown on Phase II Spacer Model

6. THERMAL ANALYSIS

The nonlinear thermal analysis performed for the HPOTP main pump housing converged in four iterations using the automatic ANSYS convergence criterion of 1°. Temperature distributions for Section AA of the primary turbine, Section DD of the secondary turbine and Section NN of the primary oxidizer drain systems are shown in Figures 37 through 42 for the pump housing and Phase II bearing components. These results are used for nodal temperature input to the structural analysis presented in Section 7. Large thermal gradients are indicated at the reflector cavity interface for Section AA of the primary turbine drain system (Figure 37).

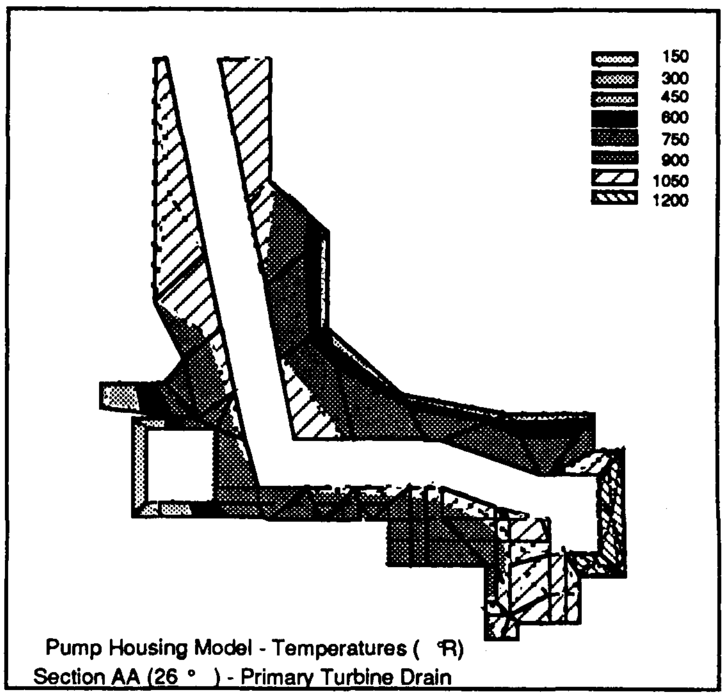

Figure 37 Temperature Distribution in HPOTP Main Pump Housing Model Section AA (26°) - Primary Turbine Drain

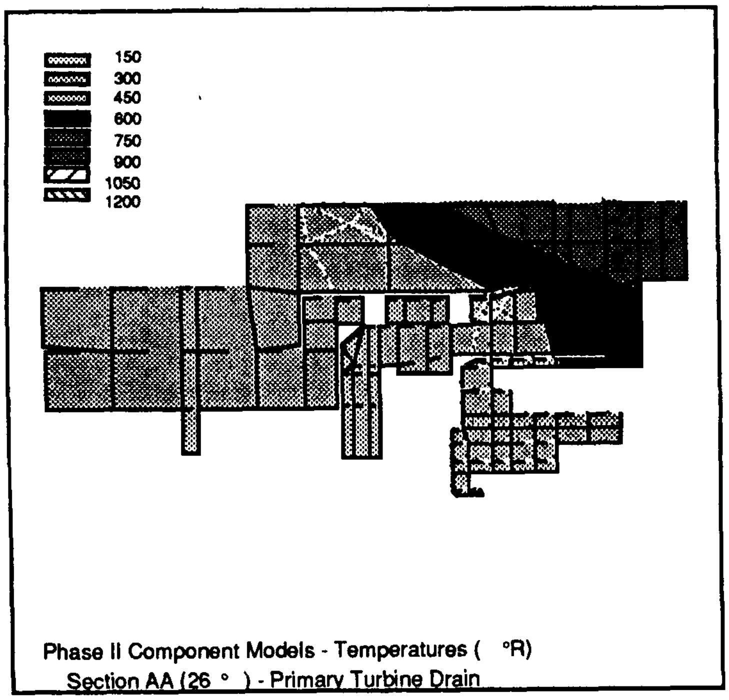

Figure 38 Temperature Distribution in HPOTP Phase II Components Section AA (26°) - Primary Turbine Drain

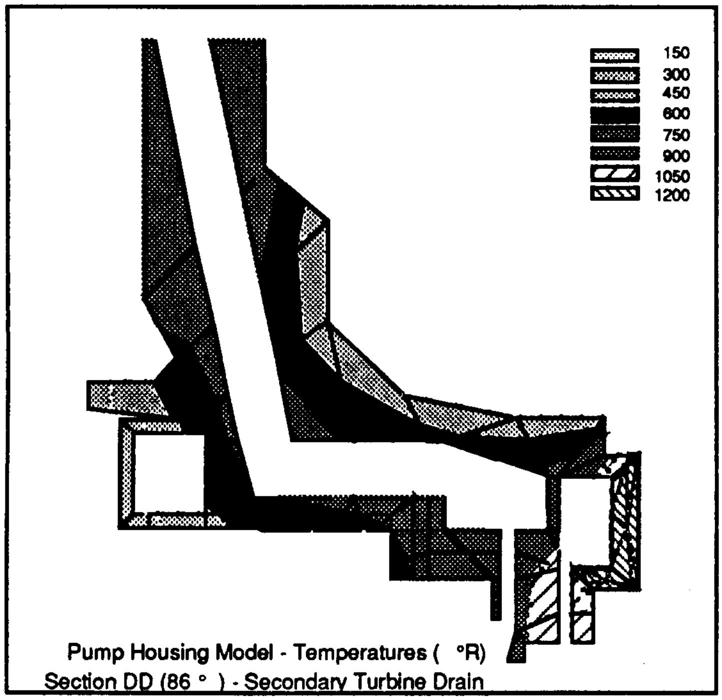

Figure 39 Temperature Distribution in HPOTP Main Pump Housing Model Section DD (86°) - Secondary Turbine Drain

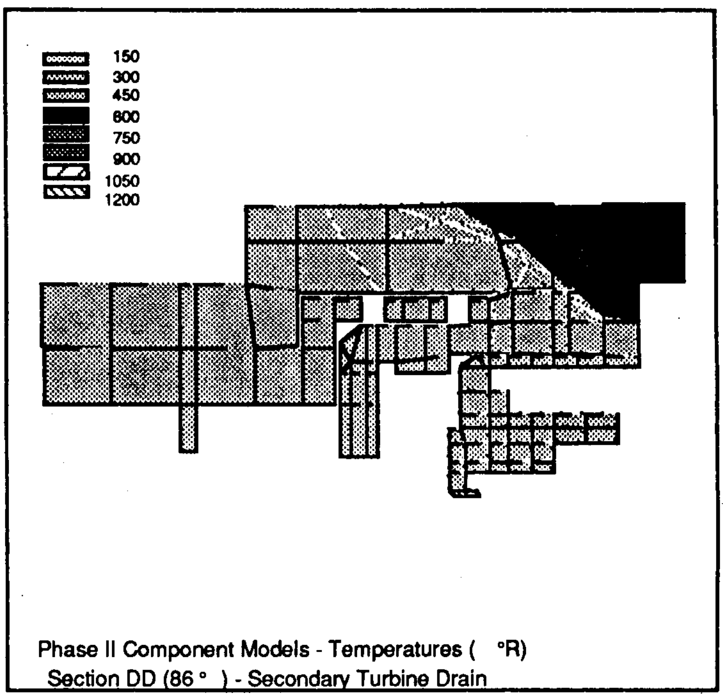

Figure 40 Temperature Distribution in HPOTP Phase II Components

Section DD (86°) - Secondary Turbine Drain

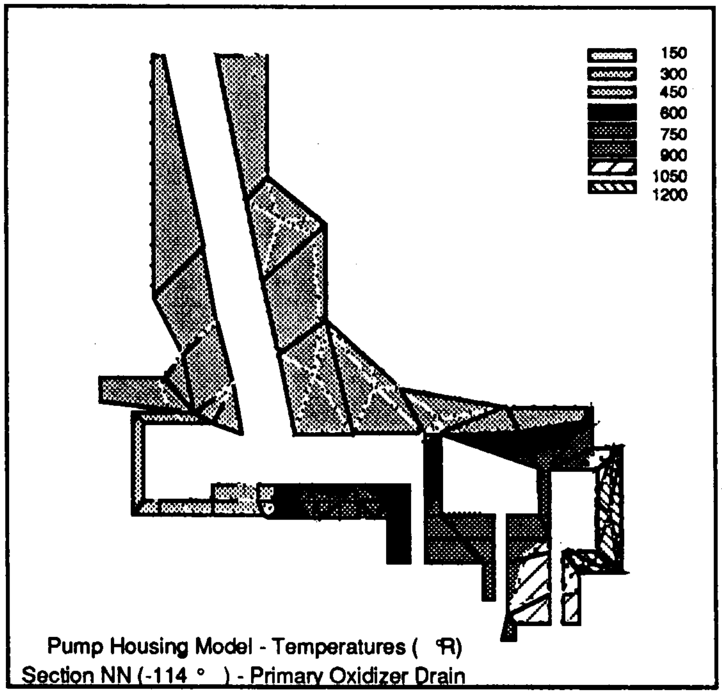

Figure 41 Temperature Distribution in HPOTP Main Pump Housing Model
Section NN (-114°) - Primary Oxidizer Drain

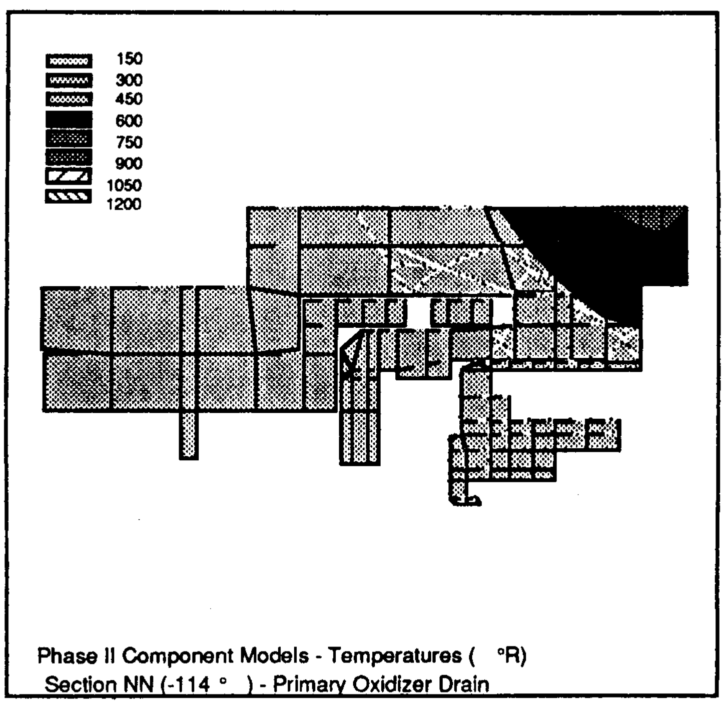

Figure 42 Temperature Distribution in HPOTP Phase II Components
Section NN (-114°) - Primary Oxidizer Drain

7. STRUCTURAL ANALYSIS

The nodal temperatures resulting from the nonlinear thermal analysis presented in Section 6 as well as the initial interference fit loads and the bolt preloads were applied to the housing model in a static analysis. The objective of this analysis was to determine the gap status between the bearing support and the axial spring cartridge (Figure 3).

The deformed shape plot for Section AA (Θ = 26°) of the primary turbine drain system is shown in Figure 43. Similar deformed shape plots for Section DD (Θ = 86°) of the secondary turbine drain system and Section NN (Θ = -114°) of the primary oxidizer drain are presented in Figures 44 and 45, respectively. To more clearly present the area of concern, these plots show the bearing support/axial spring cartridge portion of the model, but do not include the housing and drain systems. Dashed lines on the deformation plots represent the undeformed structure. For comparison, the temperature distributions from the nonlinear thermal analysis for each of these three sections are presented in Figures 37 through 42 of Section 6.

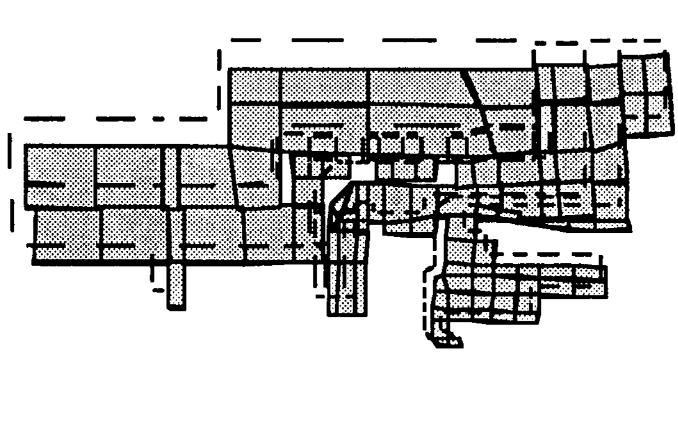

Phase II Components - Deformed Shape
Section AA (26 deg) - Primary Turbine Drain

Figure 43 Deformed Shape of HPOTP Phase II Components, Section AA (26°) - Primary Turbine Drain

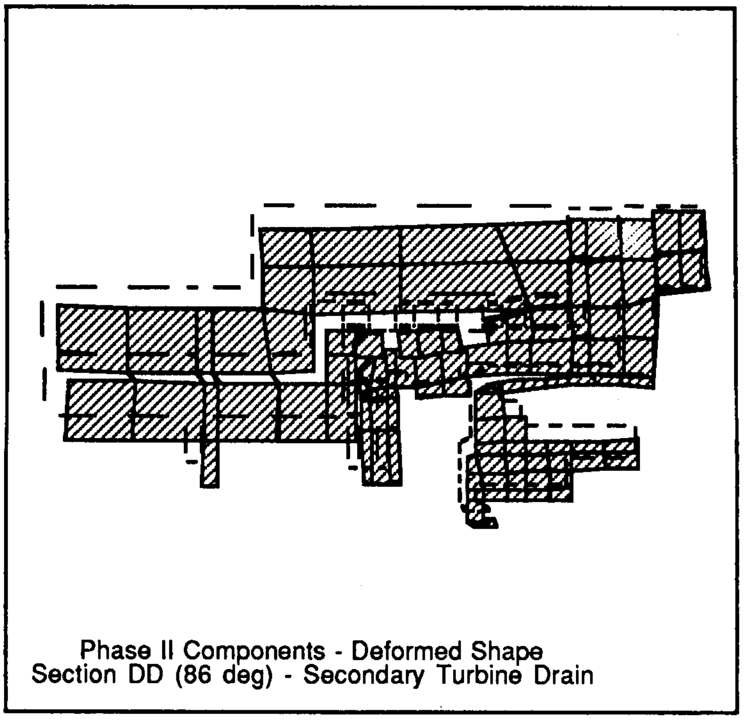

Figure 44 Deformed Shape of HPOTP Phase II Components, Section DD (86°) - Secondary Turbine Drain

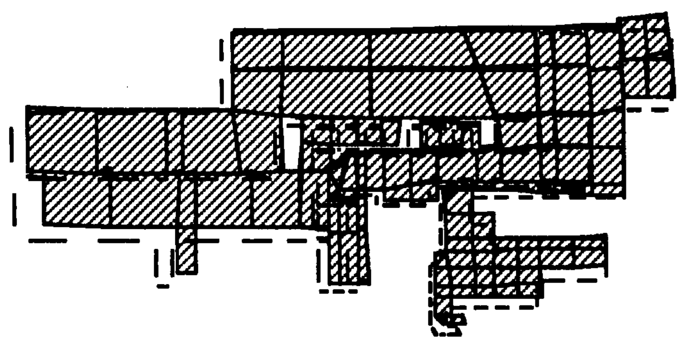

Figure 45 Deformed Shape of HPOTP Phase II Components, Section NN (-114°) - Primary Oxidizer Drain

Each of the three sections presented here yields somewhat different results. The primary drain section ($\Theta = 26°$) of Figure 43 shows movement of the bearing support/axial spring cartridge components radially inward and the contact between the support and spring cartridge. The secondary drain section ($\Theta = 86°$) of Figure 44 also shows the bearing support and axial spring cartridge components moving radially inward. However, at this cross section there is a gap between the support and the axial spring cartridge. Figure 45, the primary oxidizer drain, shows the movement of the components radially outward as well as some contact between the support and cartridge.

To focus more closely on the question of contact between the bearing support and the axial spring cartridge, the final condition of the gap elements (STIF52) modeled at this interface must be considered. As shown in Figure 7, gap elements are modeled at four places along the interface. There are two gap elements that correspond to Bearing 3 ($z = 15.165$ and $z = 15.598$) and two that correspond to Bearing 4 ($z = 15.698$ and $z = 16.065$). These gap elements are modeled in 10° increments around the circumference of the interface with an initial gap size of 0.0014 in.

The deformation of the bearing support and the axial spring cartridge causes contact between the bearing support inner surface and the outer surface of the axial spring cartridge in some locations around the circumference. Gap status for each of these gap elements is depicted in the diagrams of Figures 46 through 47. Here the inner ring represents the outer circumference of the axial spring cartridge and each x represents the corresponding nodes on the inner circumference of the bearing support. These diagrams show interference for several theta ranges: $-9° < \Theta < 21°$, $151° < \Theta < 181°$ and $251° < \Theta < 291°$. Figures 50 and 51 present gap size versus theta for the bearing support/axial spring cartridge interface. At these points of contact the bearing support transmits a normal force to the axial spring cartridge. These forces are displayed in Figures 52 through 57.

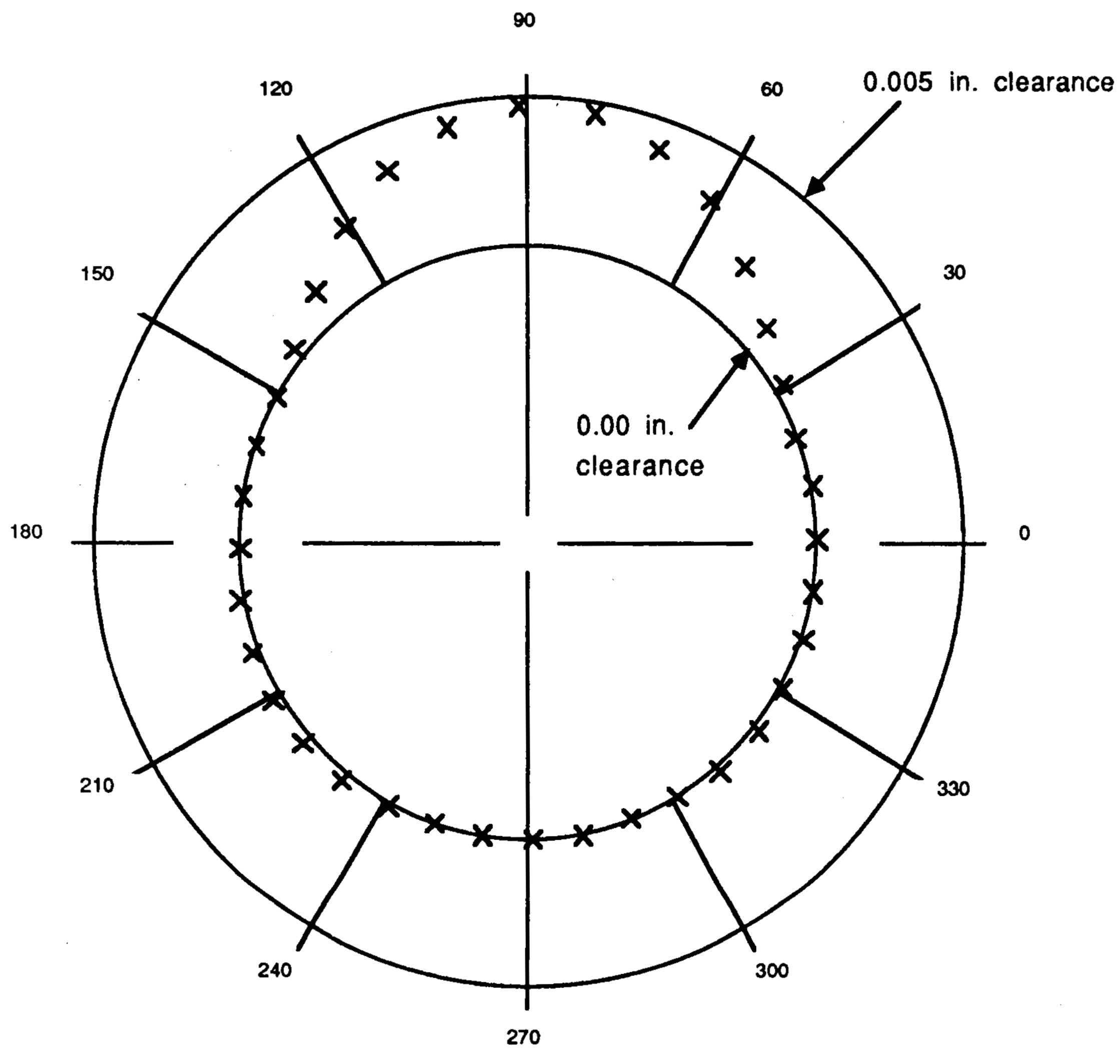

Figure 46 Node Locations of Bearing Support Inner Circumference Relative to the Axial Spring Cartridge Outer Circumference (Clearance = 0.00) at z = 15.165 (Bearing 3)

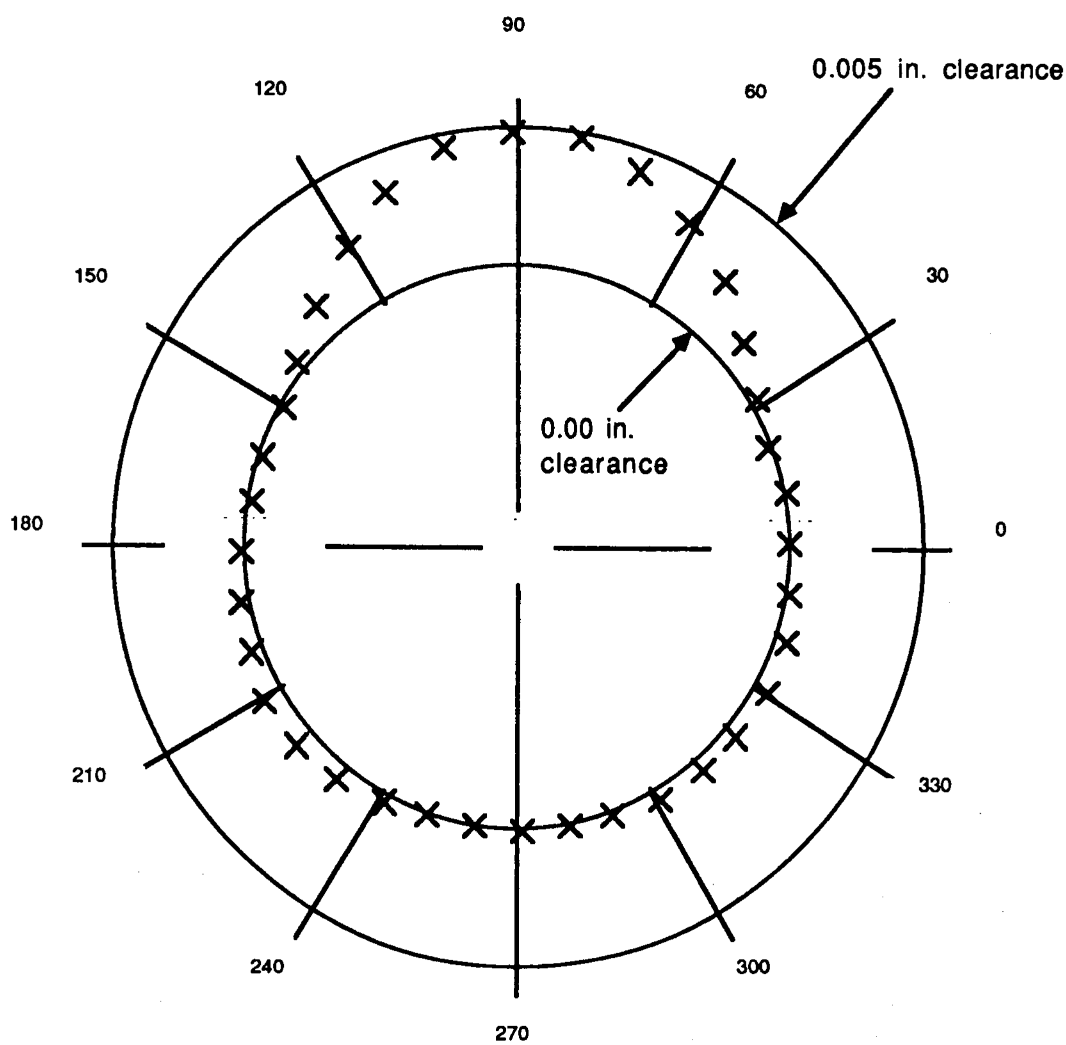

Figure 47 Node Locations of Bearing Support Inner Circumference Relative to the Axial Spring Cartridge Outer Circumference (Clearance = 0.00) at z = 15.598 (Bearing 3)

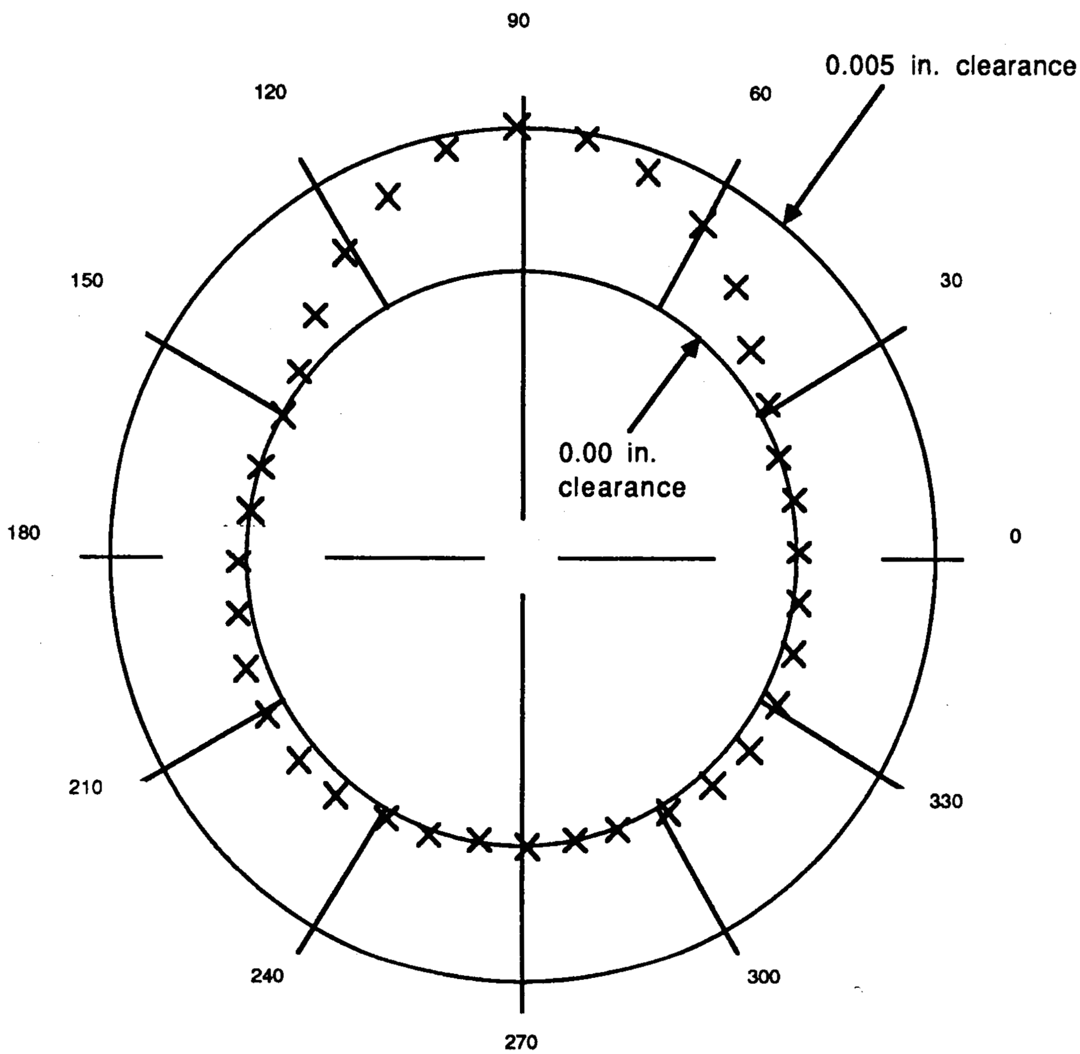

Figure 48 Node Locations of Bearing Support Inner Circumference Relative to the Axial Spring Cartridge Outer Circumference (Clearance = 0.00) at z = 15.698 (Bearing 4)

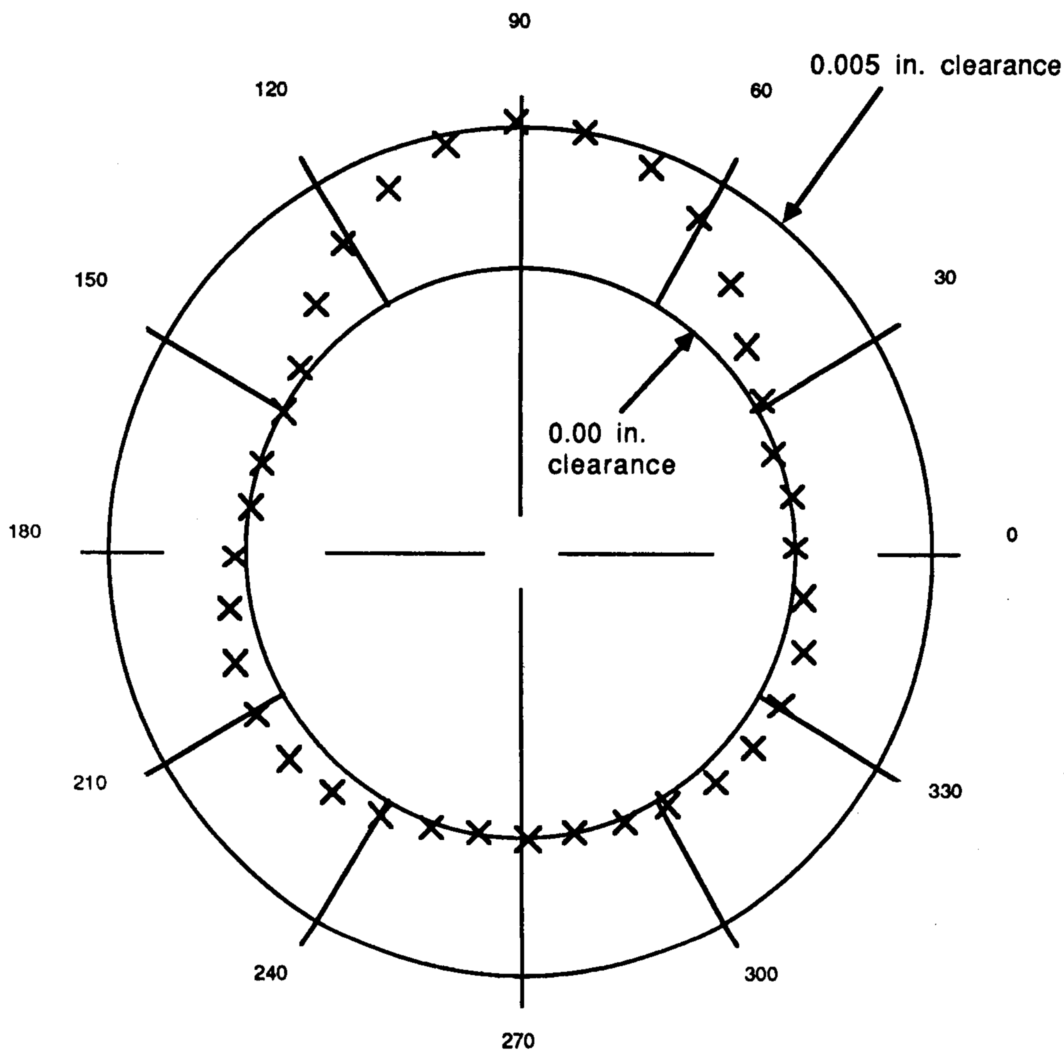

Figure 49 Node Locations of Bearing Support Inner Circumference Relative to the Axial Spring Cartridge Outer Circumference (Clearance = 0.00) at z = 16.065 (Bearing 4)

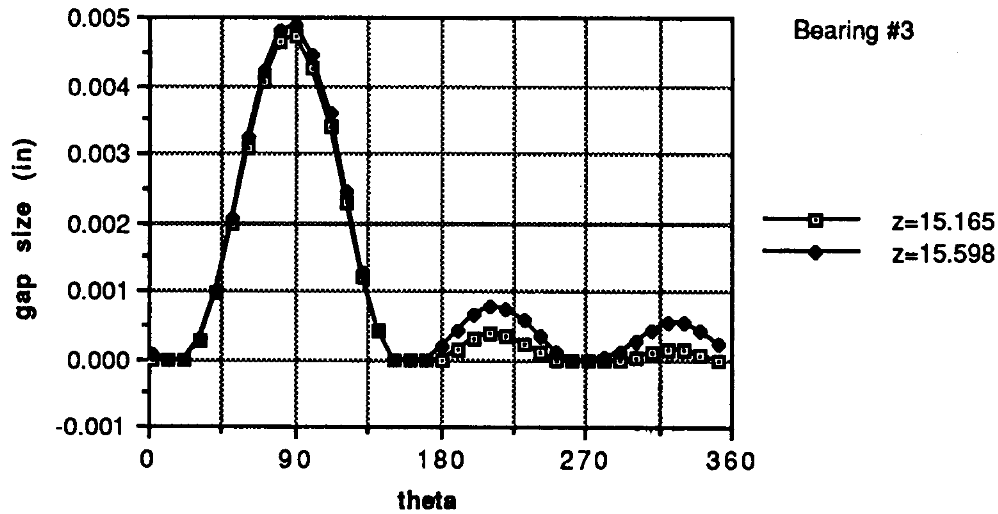

Figure 50 Gap Size versus Theta for the Nodes Corresponding to Bearing 3

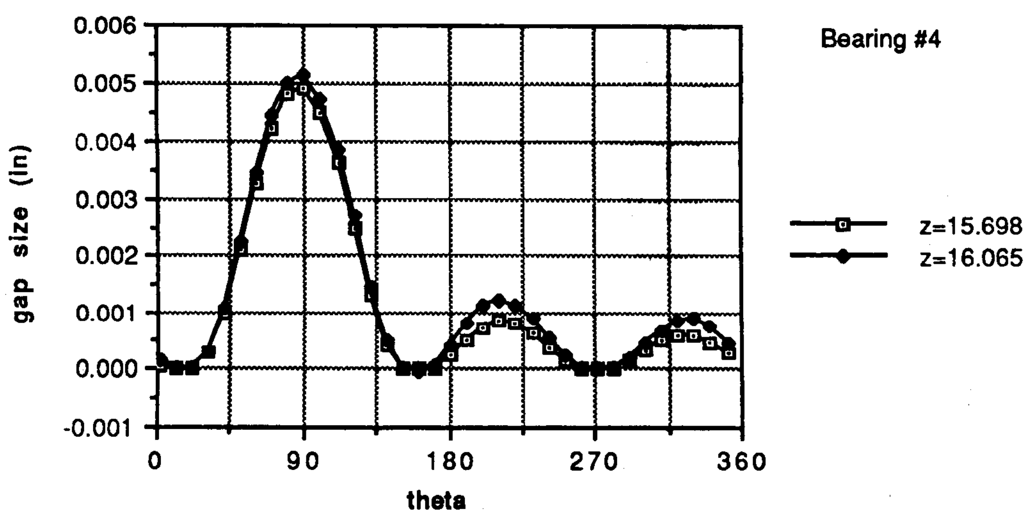

Figure 51 Gap Size versus Theta for the Nodes Corresponding to Bearing 4

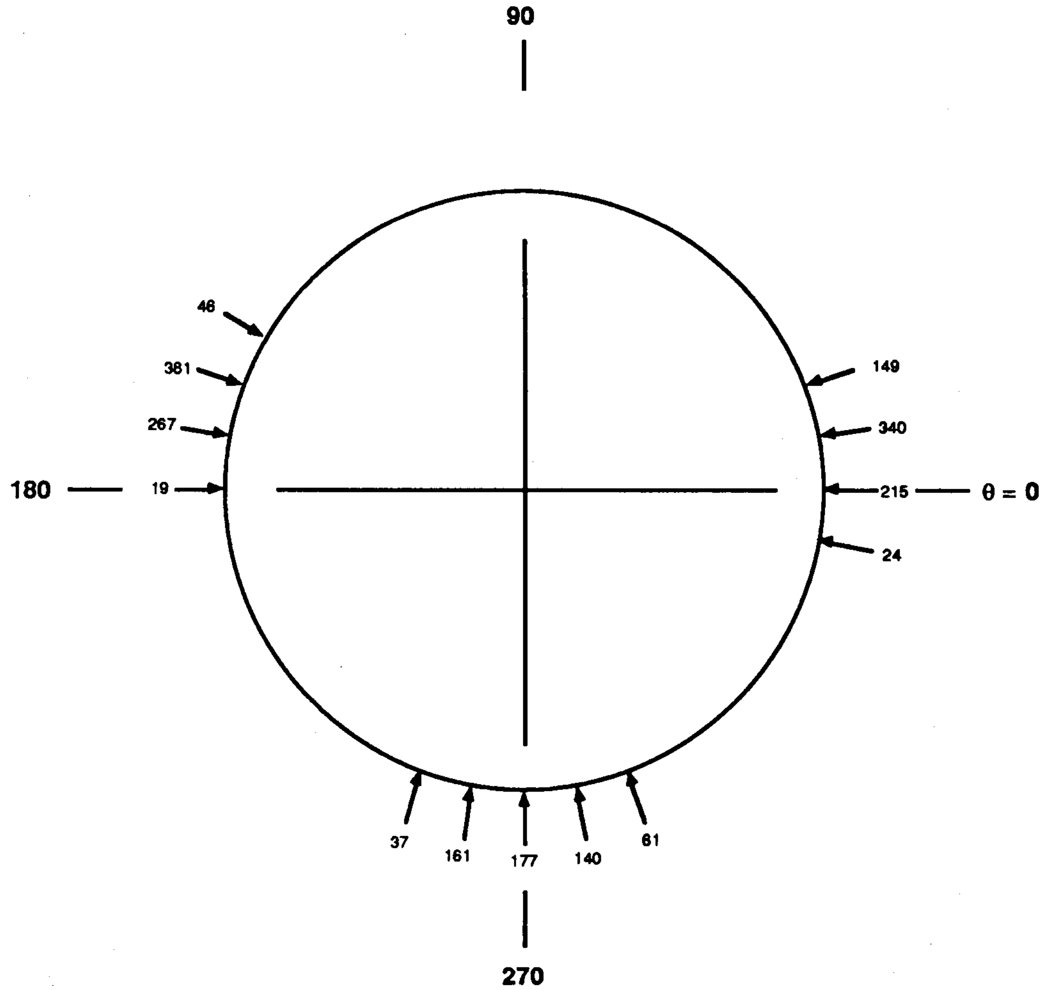

Figure 52 Normal Forces (lb) Transmitted from the Bearing Support to the Axial Spring Cartridge at z = 15.165 (Bearing 3)

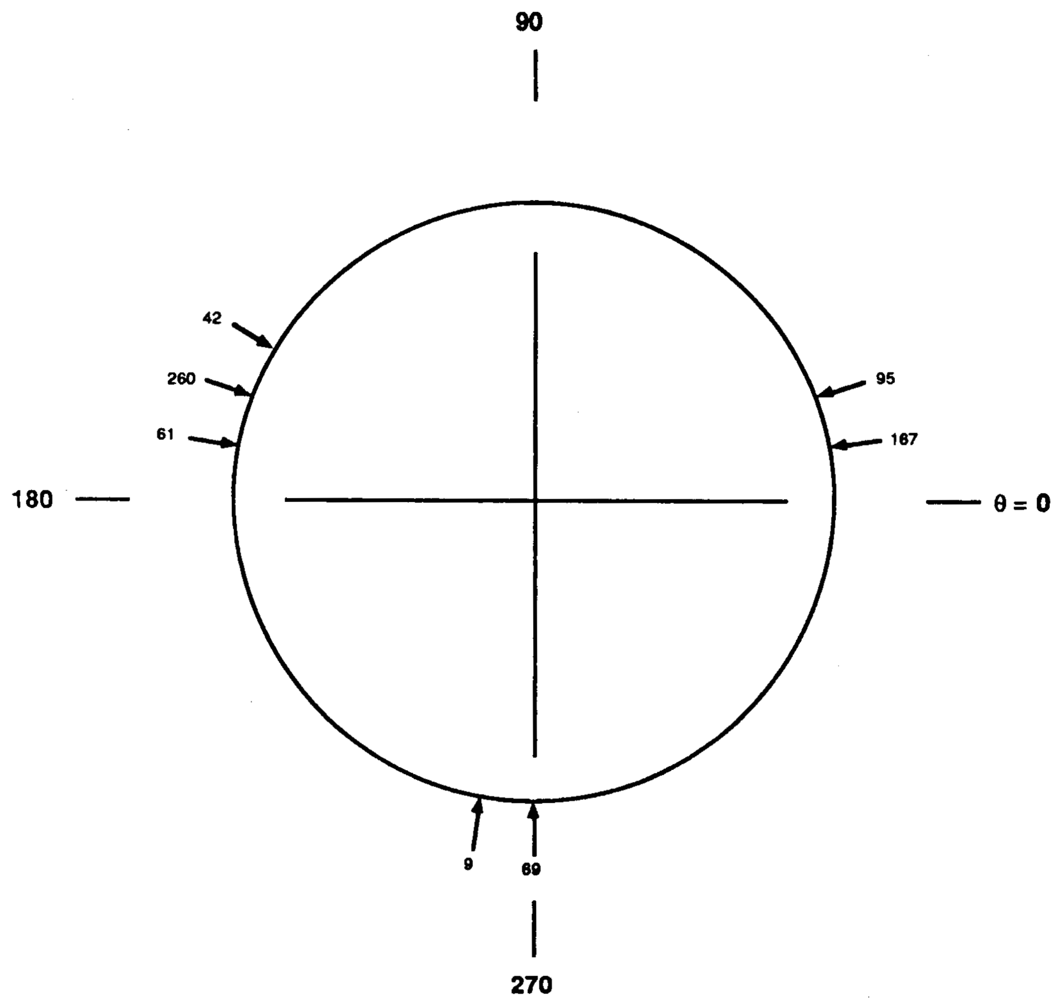

Figure 53 Normal Forces (lb) Transmitted from the Bearing Support to the Axial Spring Cartridge at z = 15.598 (Bearing 3)

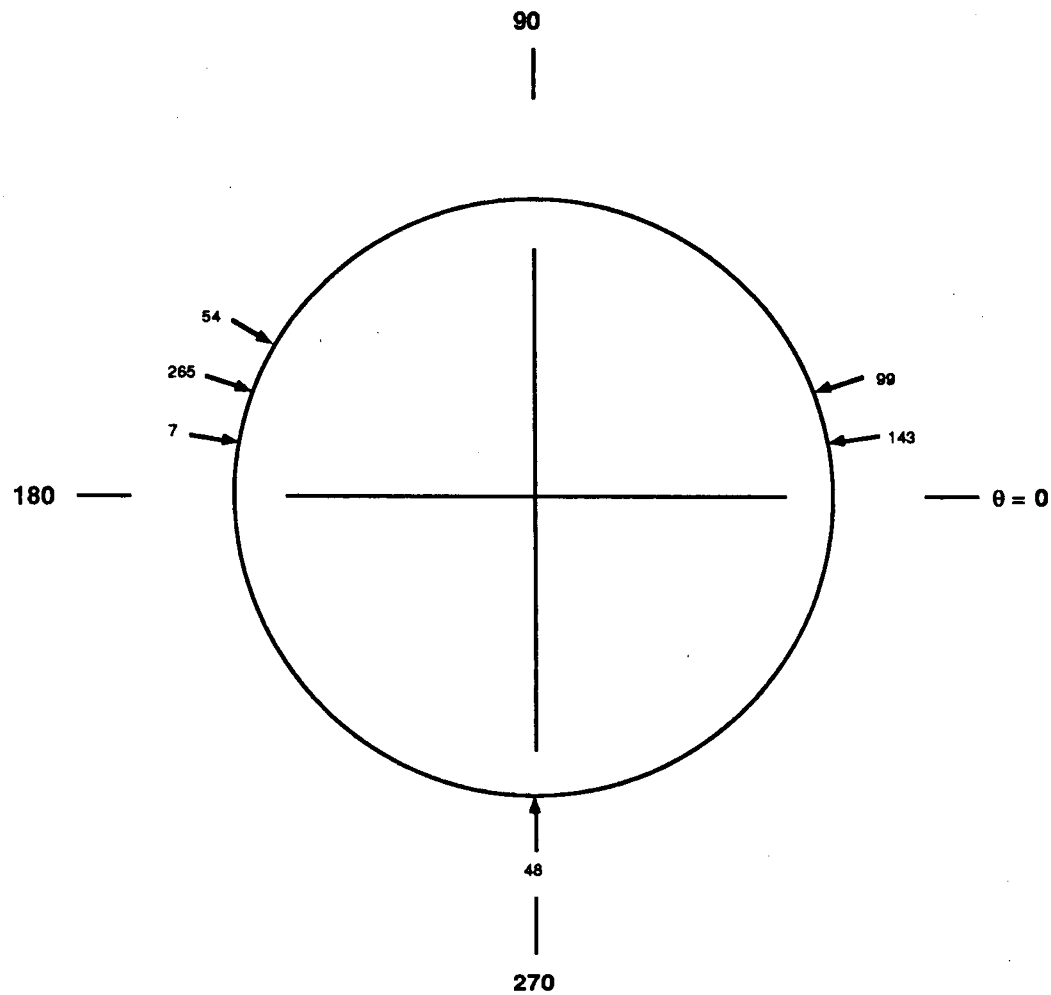

Figure 54 Normal Forces (lb) Transmitted from the Bearing Support to the Axial Spring Cartridge at z = 15.698 (Bearing 4)

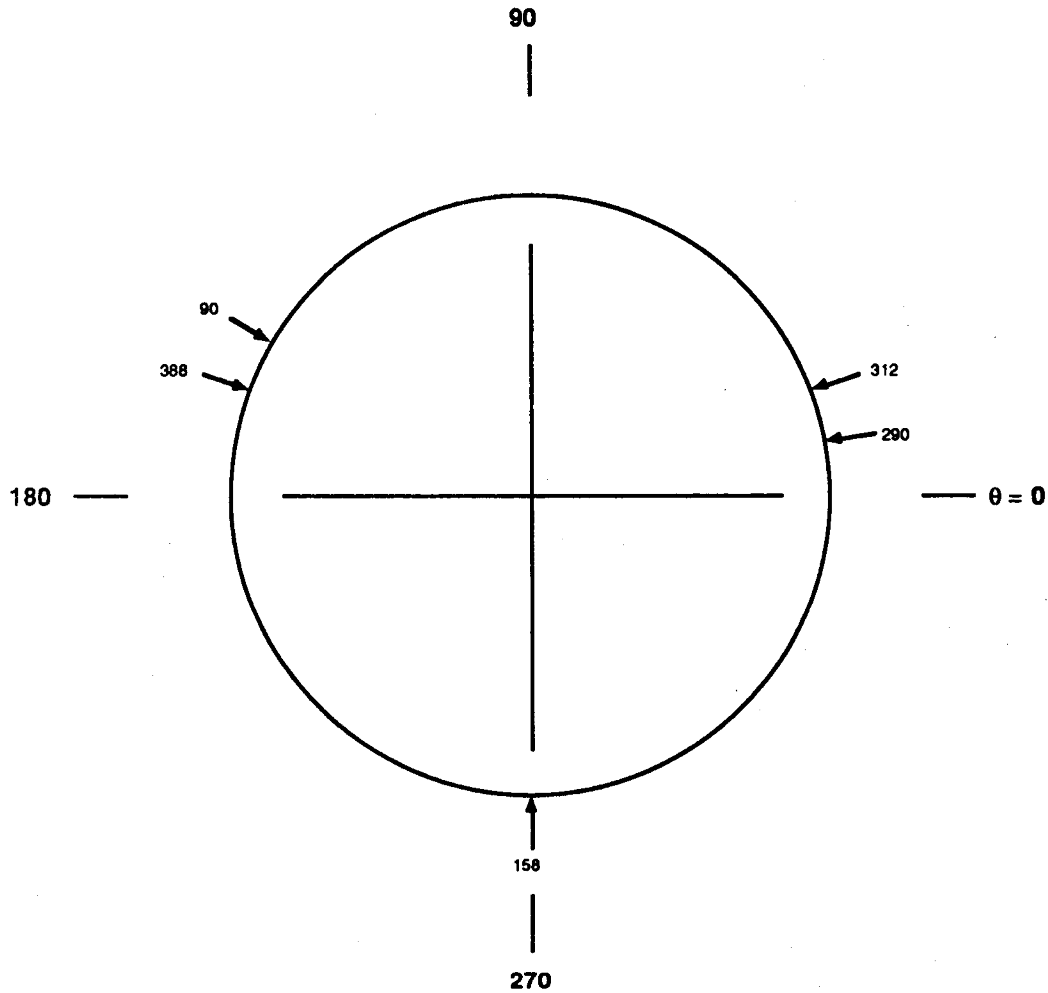

Figure 55 Normal Forces (lb) Transmitted from the Bearing Support to the Axial Spring Cartridge at z = 16.065 (Bearing 4)

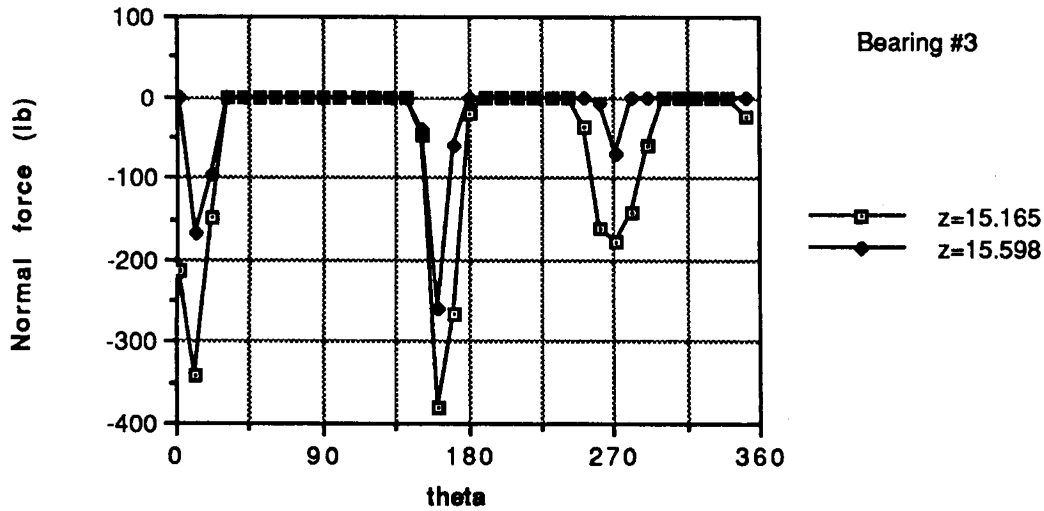

Figure 56 Normal Force versus Theta for the Nodes Corresponding to Bearing 3

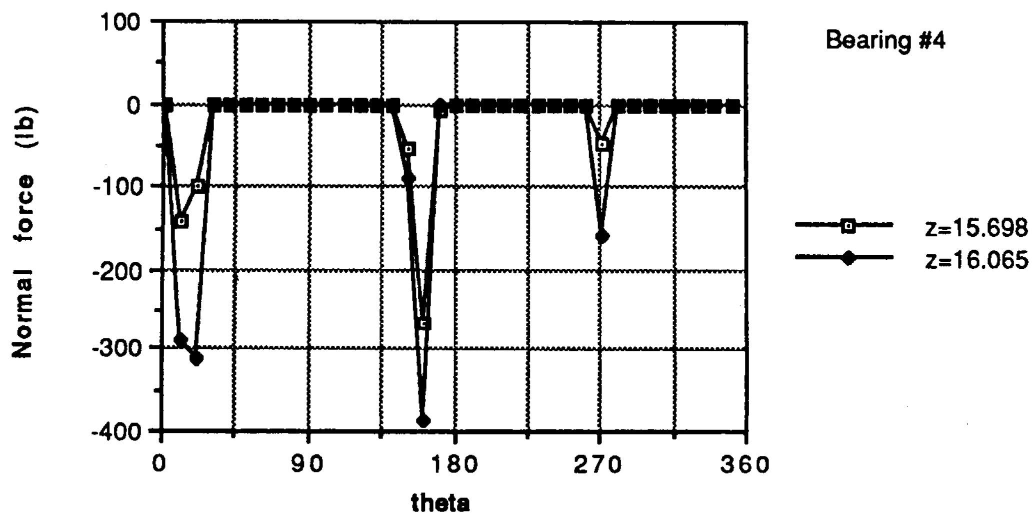

Figure 57 Normal Force versus Theta for the Nodes Corresponding to Bearing 4

8. CONCLUSIONS AND RECOMMENDATIONS

This analysis of the HPOTP main pump housing assembly reveals some contact at the bearing support/axial spring cartridge interface under current loading conditions. This contact could prevent the axial spring cartridge from performing properly and therefore could cause turbine shaft hang-up.

It should be noted that the stiffness of the outer bearing race has not been accounted for in this analysis. It is believed that this influence could be significant and should be considered in any later analysis. The pressure inside the manifold and drain systems of the pump housing was also excluded from this analysis as its influence on the bearing support/axial spring cartridge interface was assumed to be negligible.

Appendix A

HPOTP MAIN PUMP HOUSING ASSEMBLY SUBMODELS

Appendix A
HPOTP MAIN PUMP HOUSING ASSEMBLY SUBMODELS

Sector submodels of the HPOTP main pump housing were developed to obtain better localized displacement results if necessary. Submodeling eliminates the need to regenerate the entire global pump housing model with a finer mesh. Instead, finer models around regions of interest are generated.

The sector submodels were constructed using the I-DEAS Supertab mechanical CAE software running on a SUN 3/60 workstation. The submodels were developed using a top-down approach in which global solid models of the pump housing and drainage system were used as the starting point in the finite element model development. Sector solid models are cut from the global solid models. The sector solid model geometry cannot be used by the mesh generation module of Supertab. Points, curves, lines, and surfaces of the solid geometry are simplified and grouped to form subareas and subvolumes. Once the sector geometry has been prepared, mesh generation can proceed. Mesh generation is controlled by specifying the element type (4-node tetrahedrals) and element density within each control region (subareas and subvolumes) of the sector geometry. Once generated, the submodels are converted to ANSYS PREP7 data decks using the file translation facility within Supertab. The Supertab universal files used to generate the finite element submodels are available on two 1/4-inch cartridge tapes. The PREP7 data decks are then transferred to Lockheed/Huntsville VAX 11/785 using Kermit. Using the PREP7 data decks, element and node files (FILE14 and FILE15) were generated with ANSYS.

The number of nodes and elements for each sector model is given in Table A-1. Hidden line plots of each detailed sector model are shown in Figs. A-1 through A-15. The sector models are available as pairs of ANSYS element and node data files (FILE14 and FILE15). An unlabeled ASCII magnetic tape containing the sector models was created. Table A-2 lists the order in which the sector model data was written to tape.

Table A-1 NODE AND ELEMENT ESTIMATES FOR DETAILED HPOTP MAIN PUMP HOUSING SECTOR SUBMODELS

SECTION	CIRCUMFERENTIAL LOCATION, DEGREES		NODES	ELEMENTS
	from	to		
1	0	12	828	2578
2	16	38	1205	4284
3	40	52	828	2578
4	60	72	828	2578
5	80	98	920	2784
6	100	112	828	2578
7	116	176	1067	3596
8	180	192	736	2138
9	200	212	828	2578
10	220	232	828	2578
11	238	254	842	2749
12	256	268	283	712
13	270	312	914	2963
14	320	332	828	2578
15	336	352	934	2807
		TOTALS	12697	40079

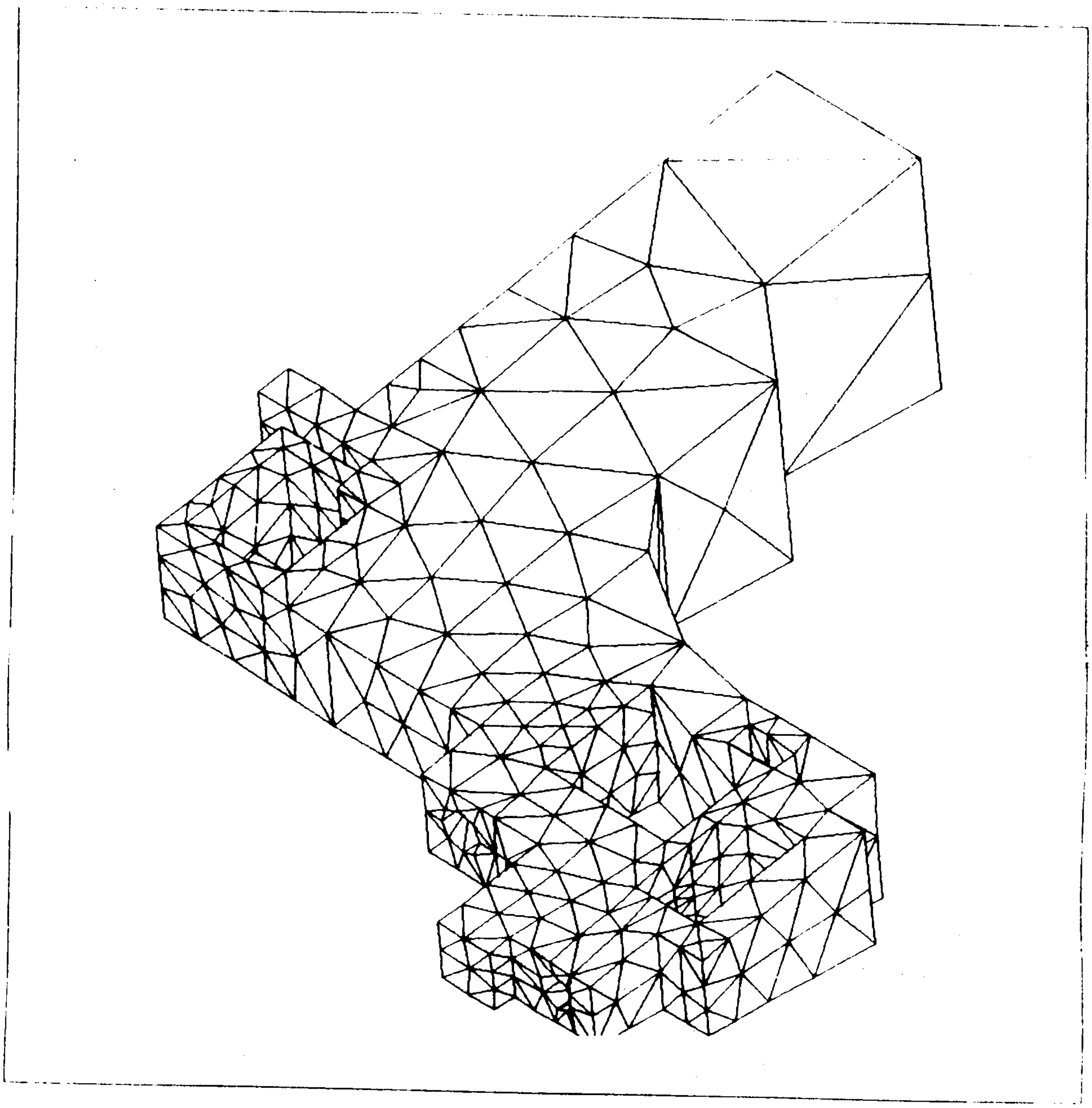

Fig. A-1 Hidden Line Plot of Detailed HPOTP Main Pump Housing Sector Model from 0 to 12°

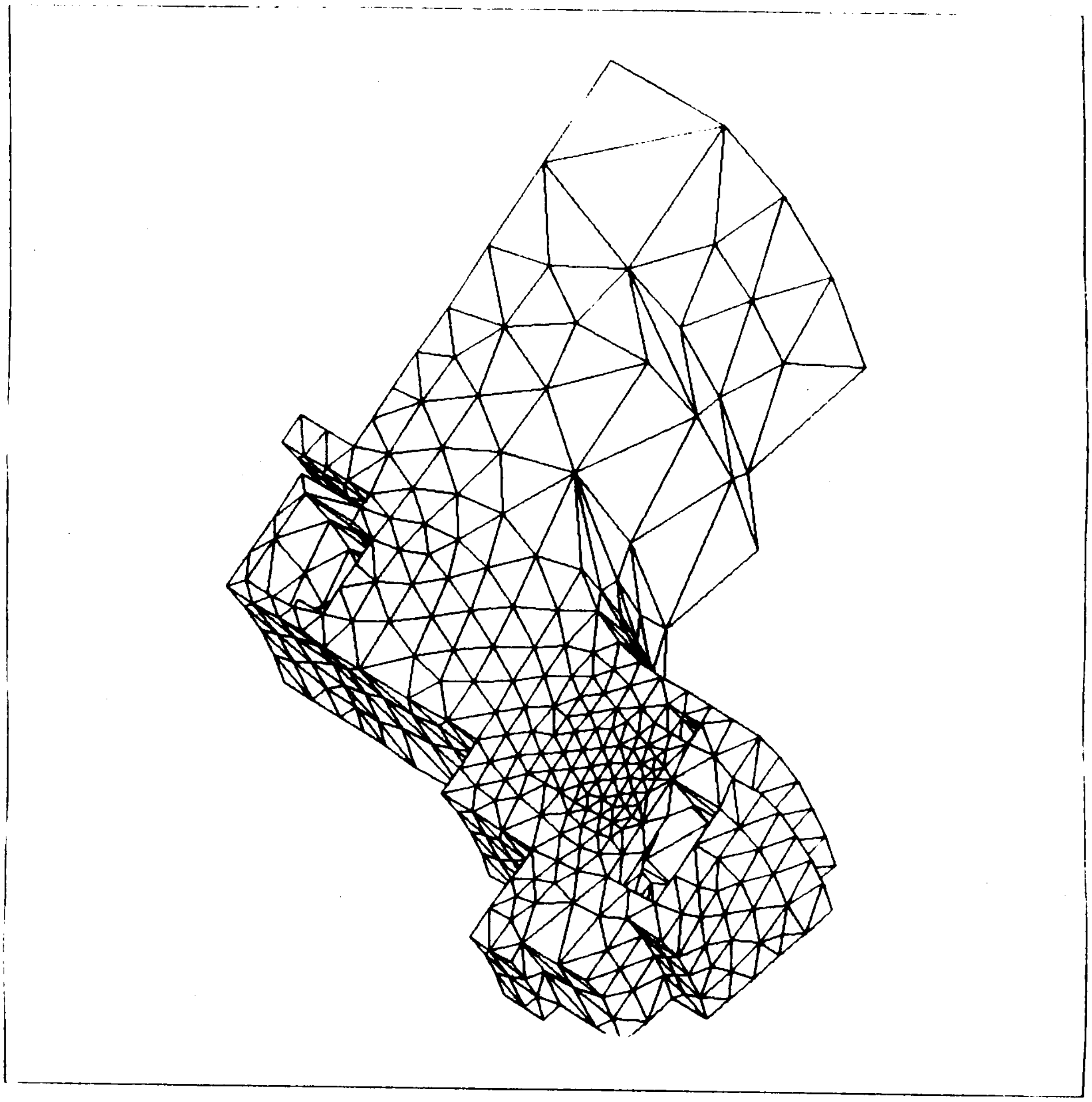

Fig. A-2 Hidden Line Plot of Detailed HPOTP Main Pump Housing Sector Model from 16 to 38°

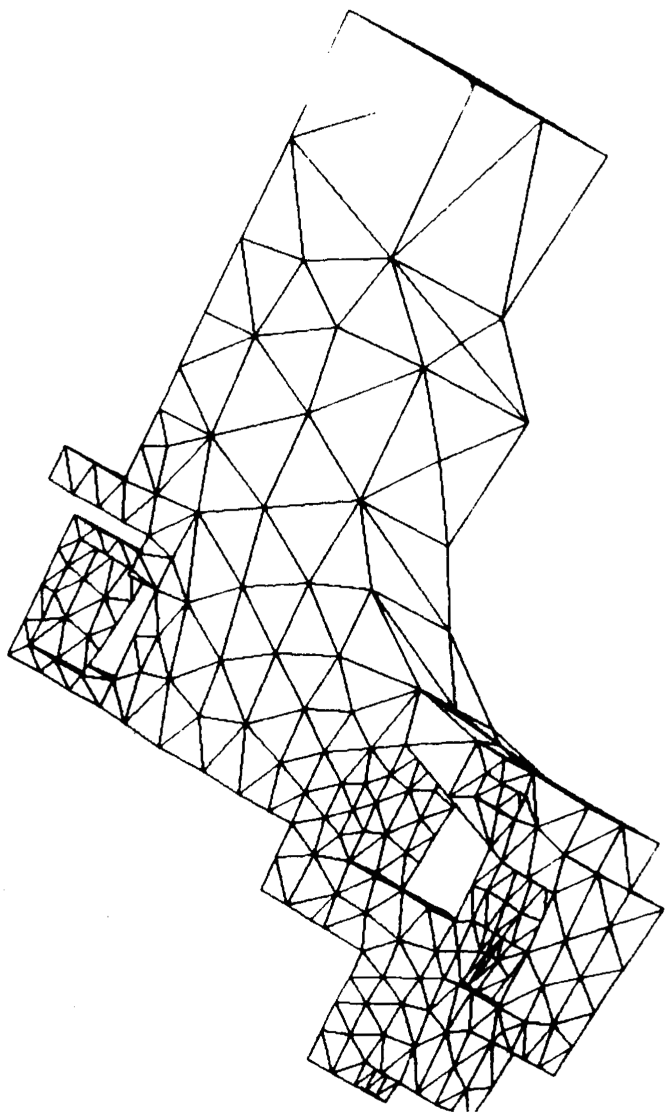

Fig. A-3 Hidden Line Plot of Detailed HPOTP Main Pump Housing Sector Model from 40 to 52°

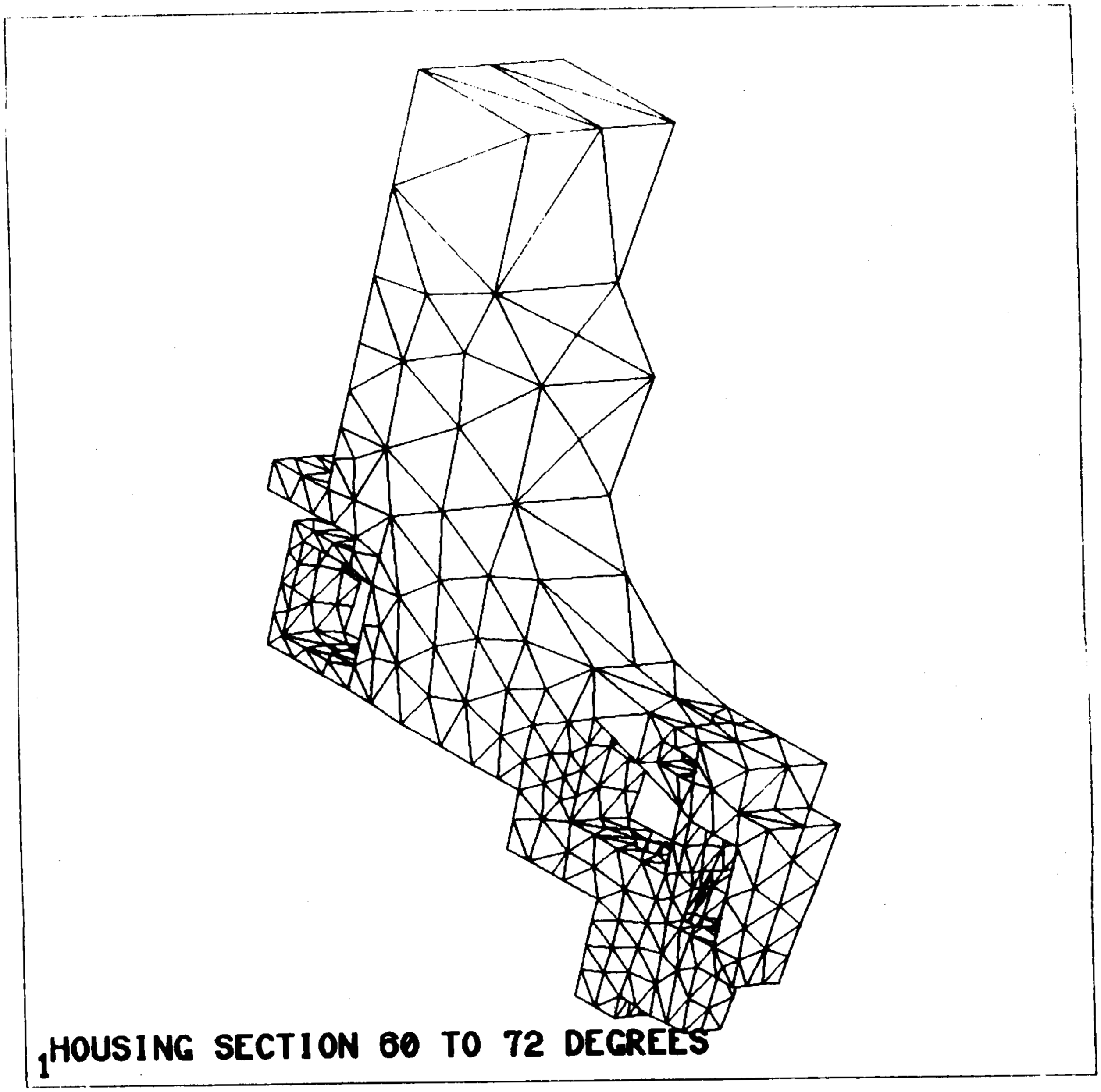

Fig. A-4 Hidden Line Plot of Detailed HPOTP Main Pump Housing Sector Model from 60 to 72°

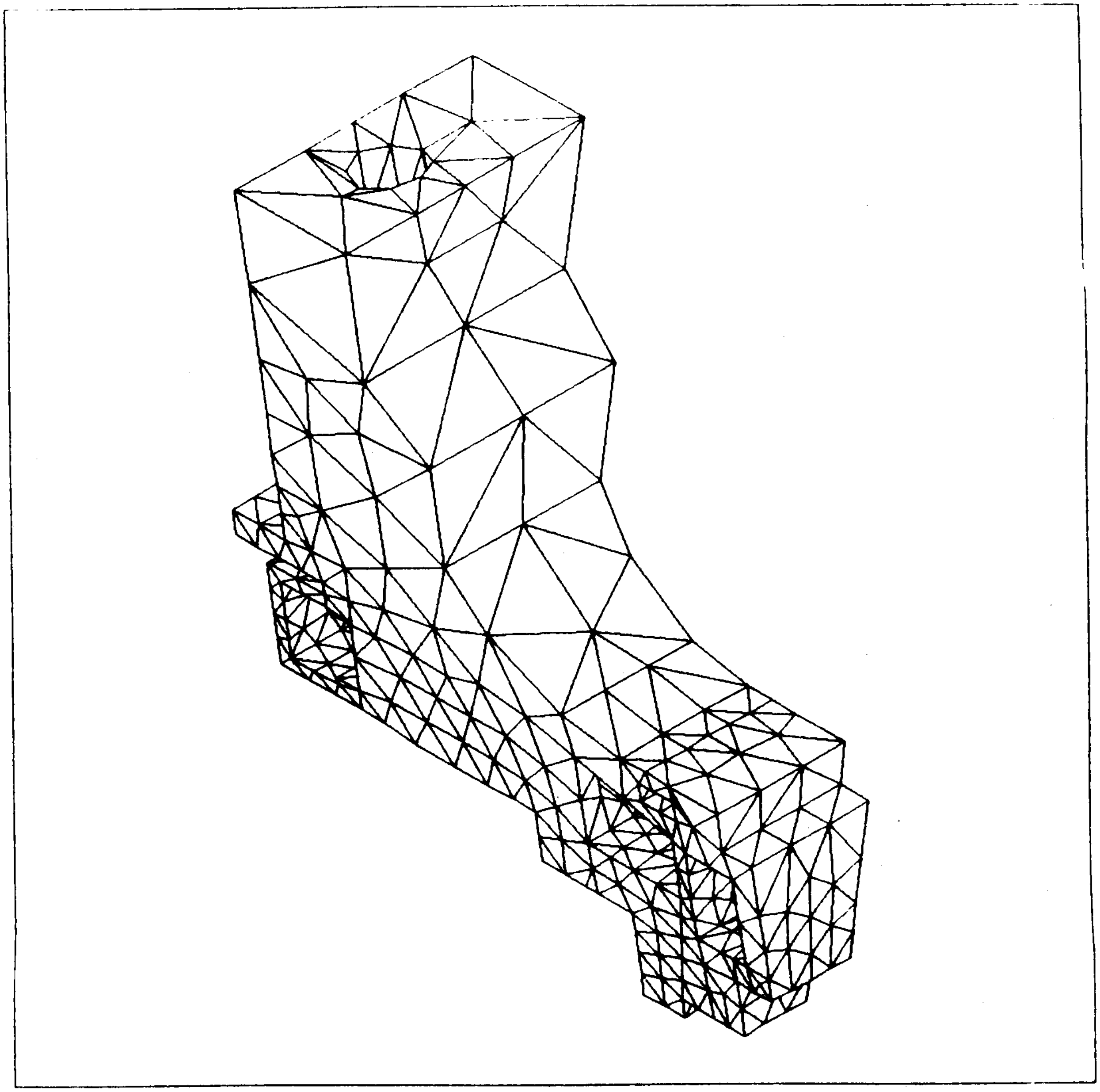

Fig. A-5 Hidden Line Plot of Detailed HPOTP Main Pump Housing Sector Model from 80 to 98°

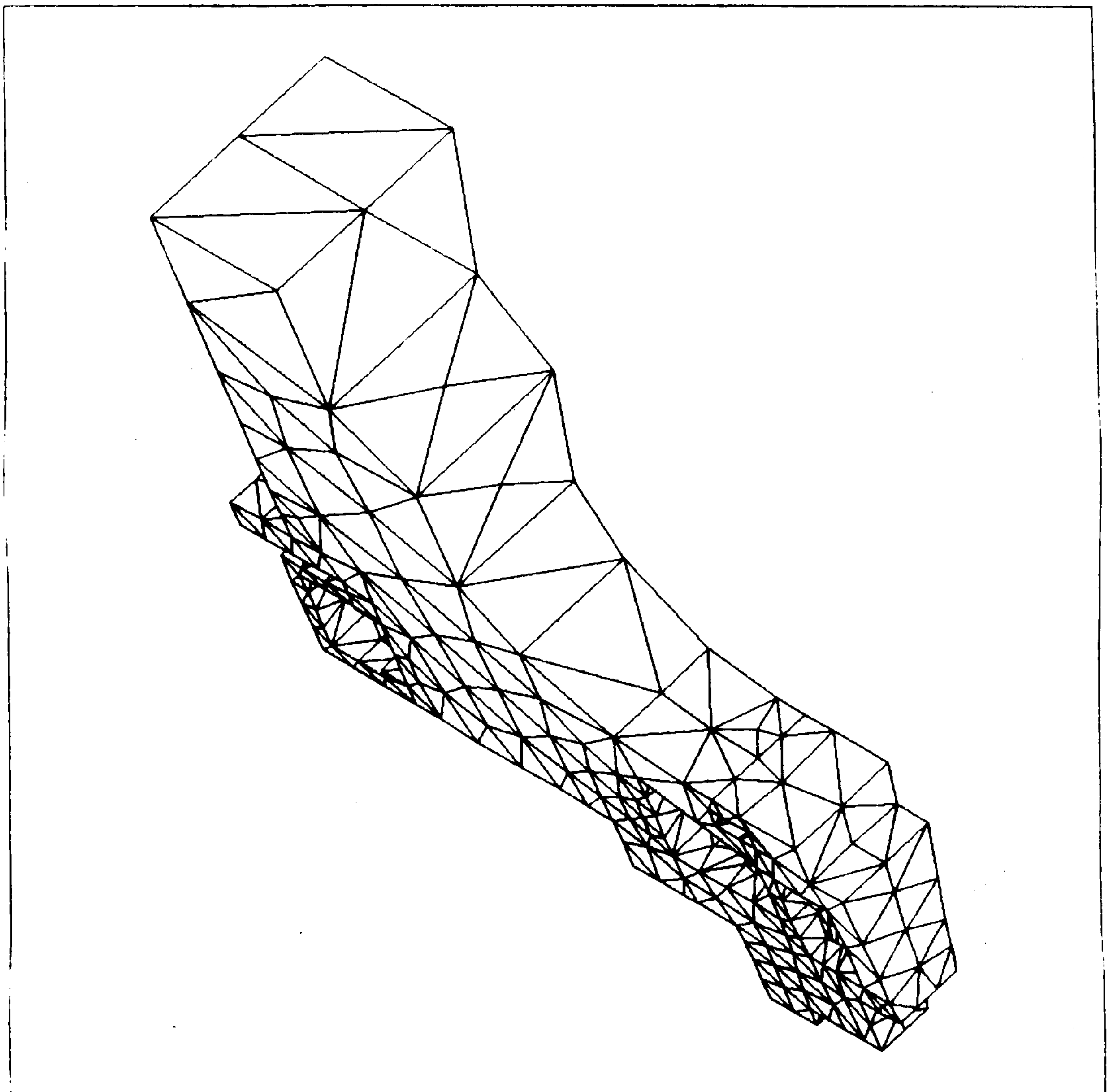

Fig. A-6 Hidden Line Plot of Detailed HPOTP Main Pump Housing Sector Model from 100 to 112°

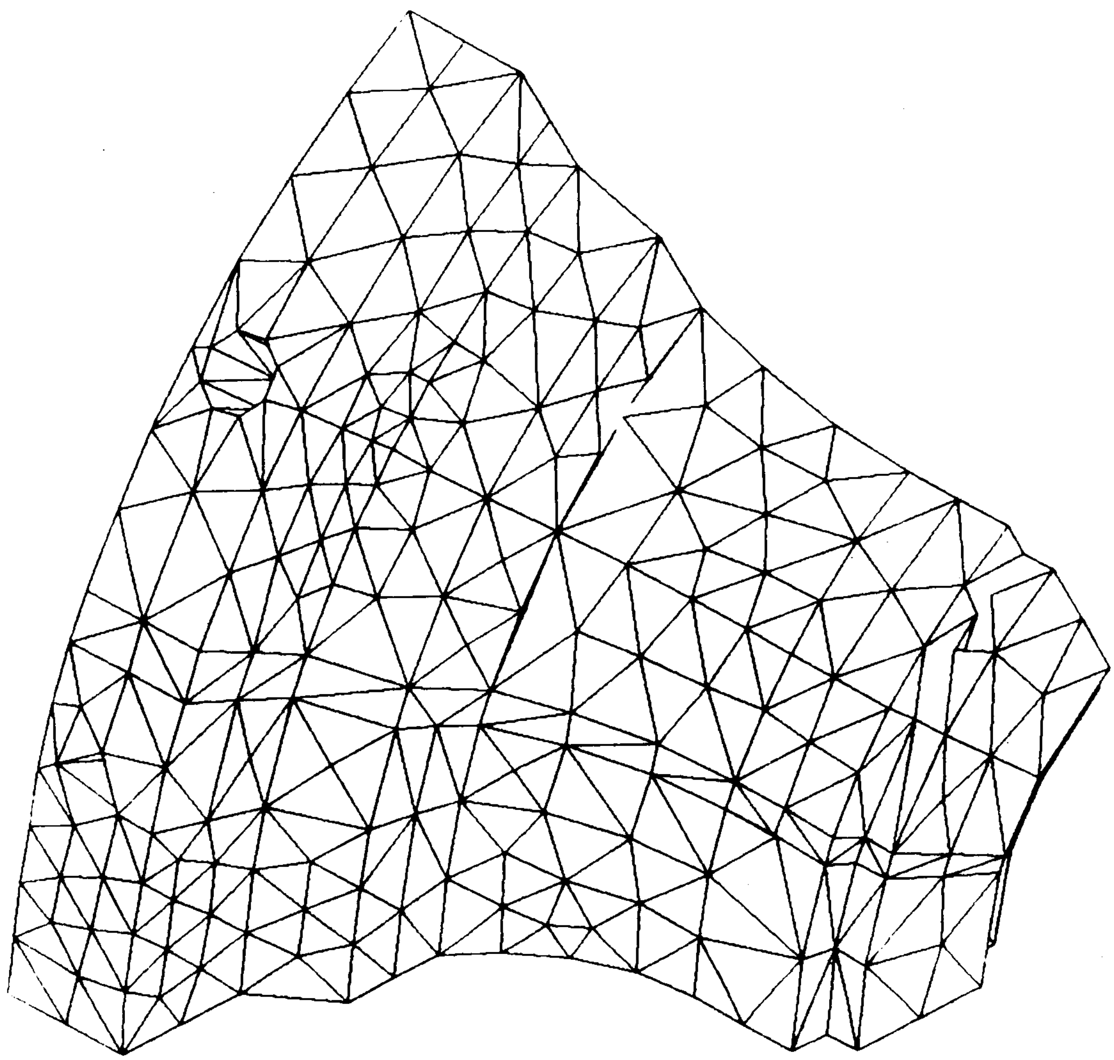

Fig. A-7 Hidden Line Plot of Detailed HPOTP Main Pump Housing Sector Model from 116 to 176°

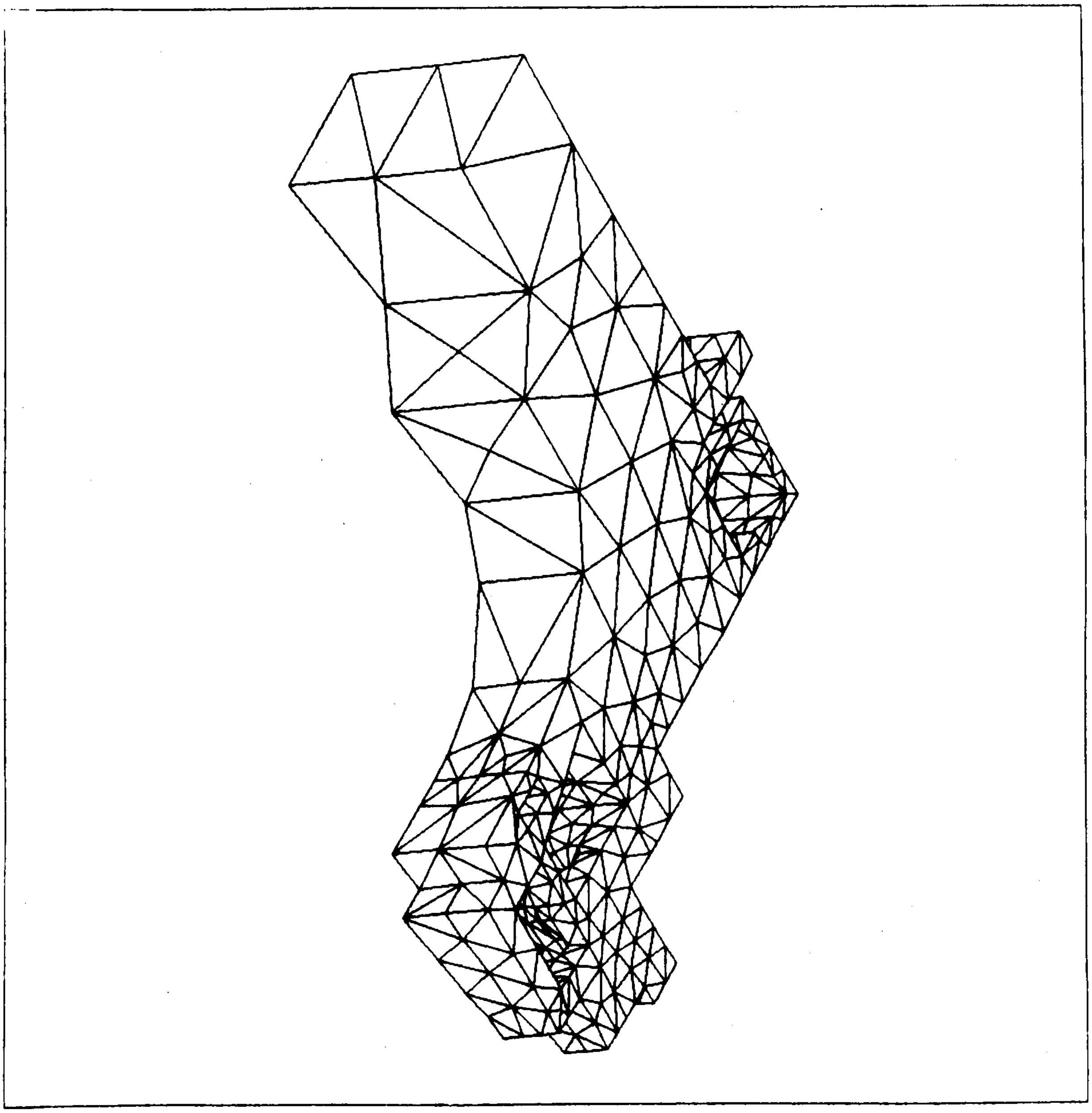

Fig. A-8 Hidden Line Plot of Detailed HPOTP Main Pump Housing Sector Model from 180 to 192°

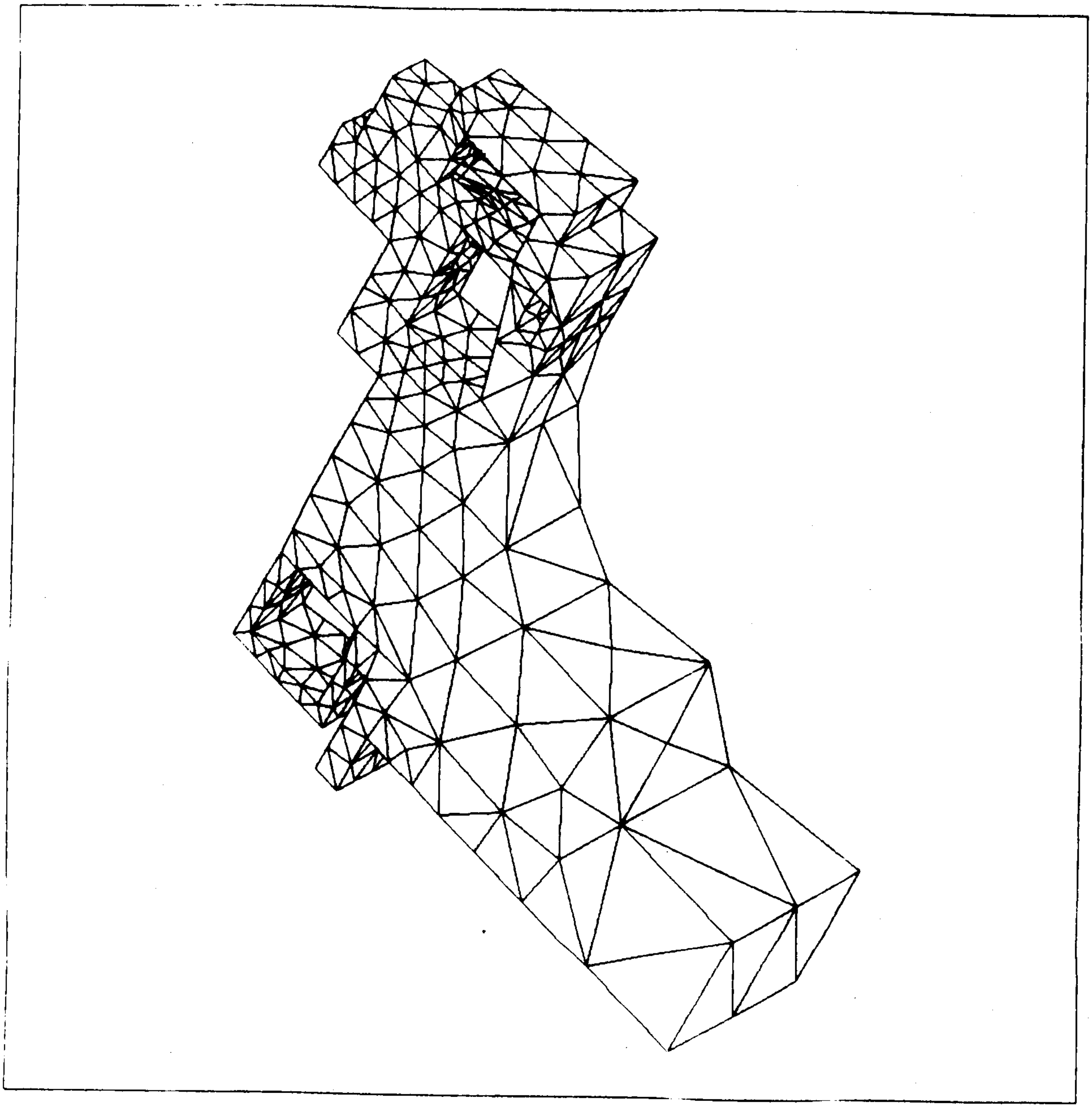

Fig. A-9 Hidden Line Plot of Detailed HPOTP Main Pump Housing Sector Model from 200 to 212°

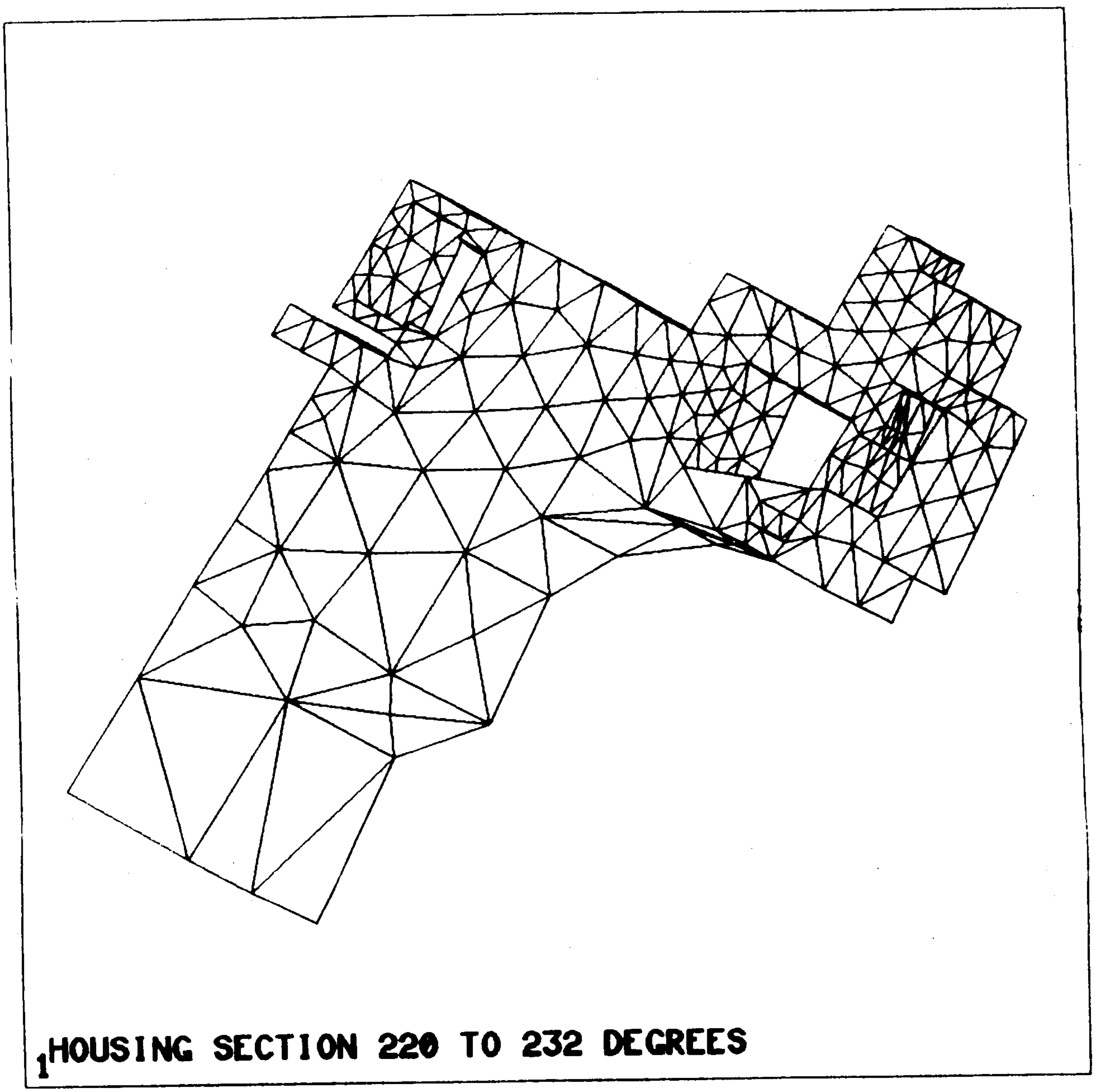

Fig. A-10 Hidden Line Plot of Detailed HPOTP Main Pump Housing Sector Model from 220 to 232°

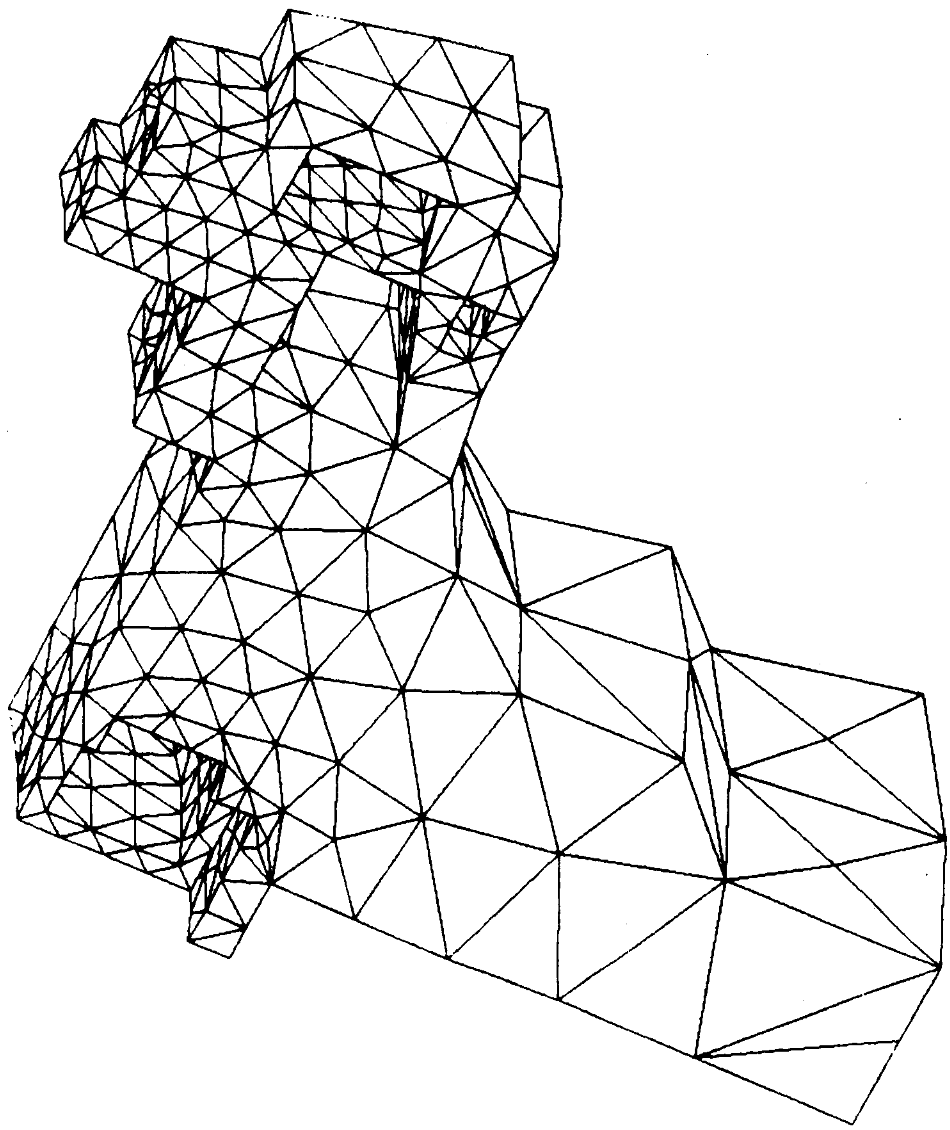

Fig. A-11 Hidden Line Plot of Detailed HPOTP Main Pump Housing Sector Model from 238 to 254°

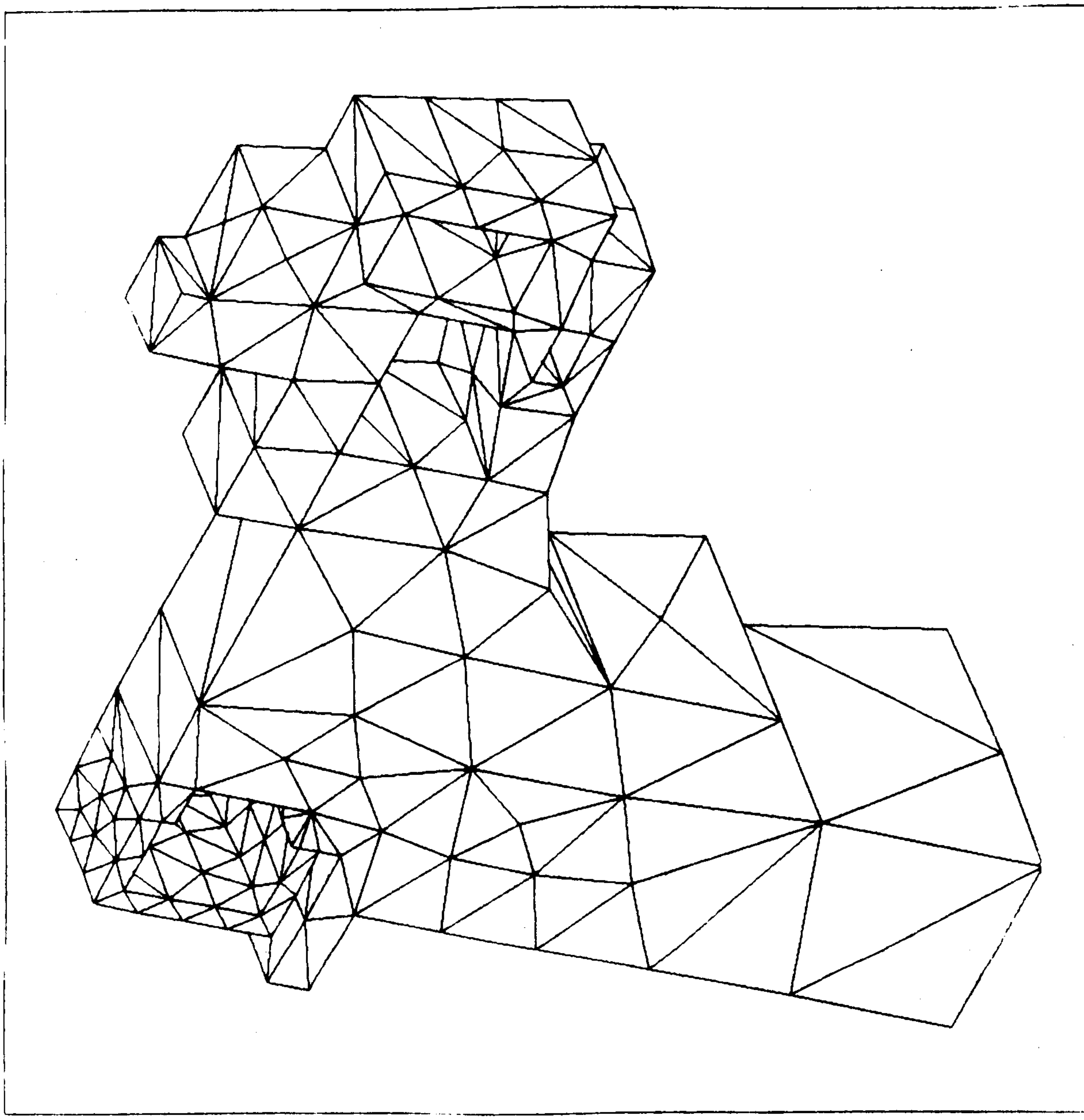

Fig. A-12 Hidden Line Plot of Detailed HPOTP Main Pump Housing Sector Model from 256 to 268°

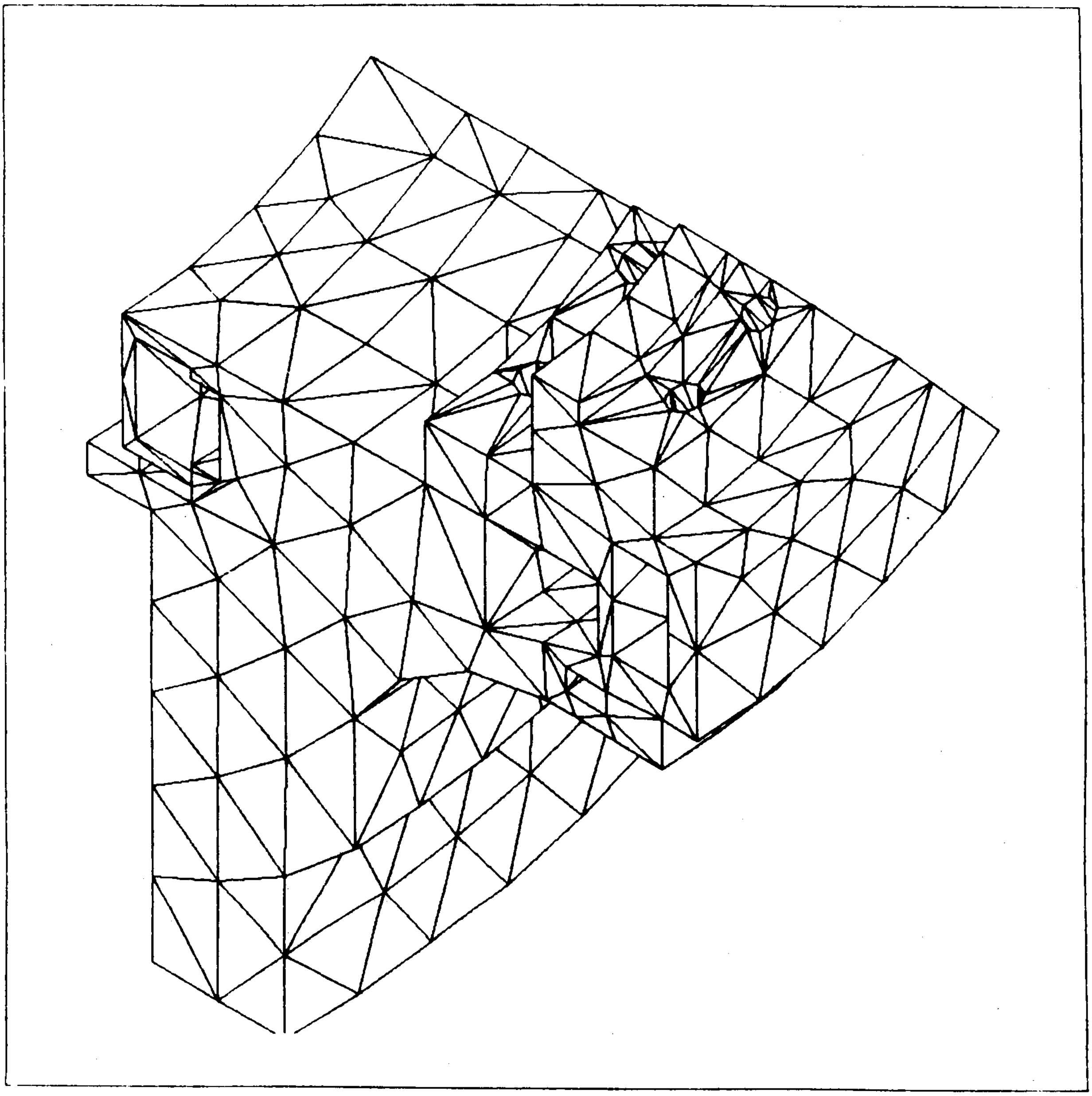

Fig. A-13 Hidden Line Plot of Detailed HPOTP Main Pump Housing Sector Model from 270 to 312°

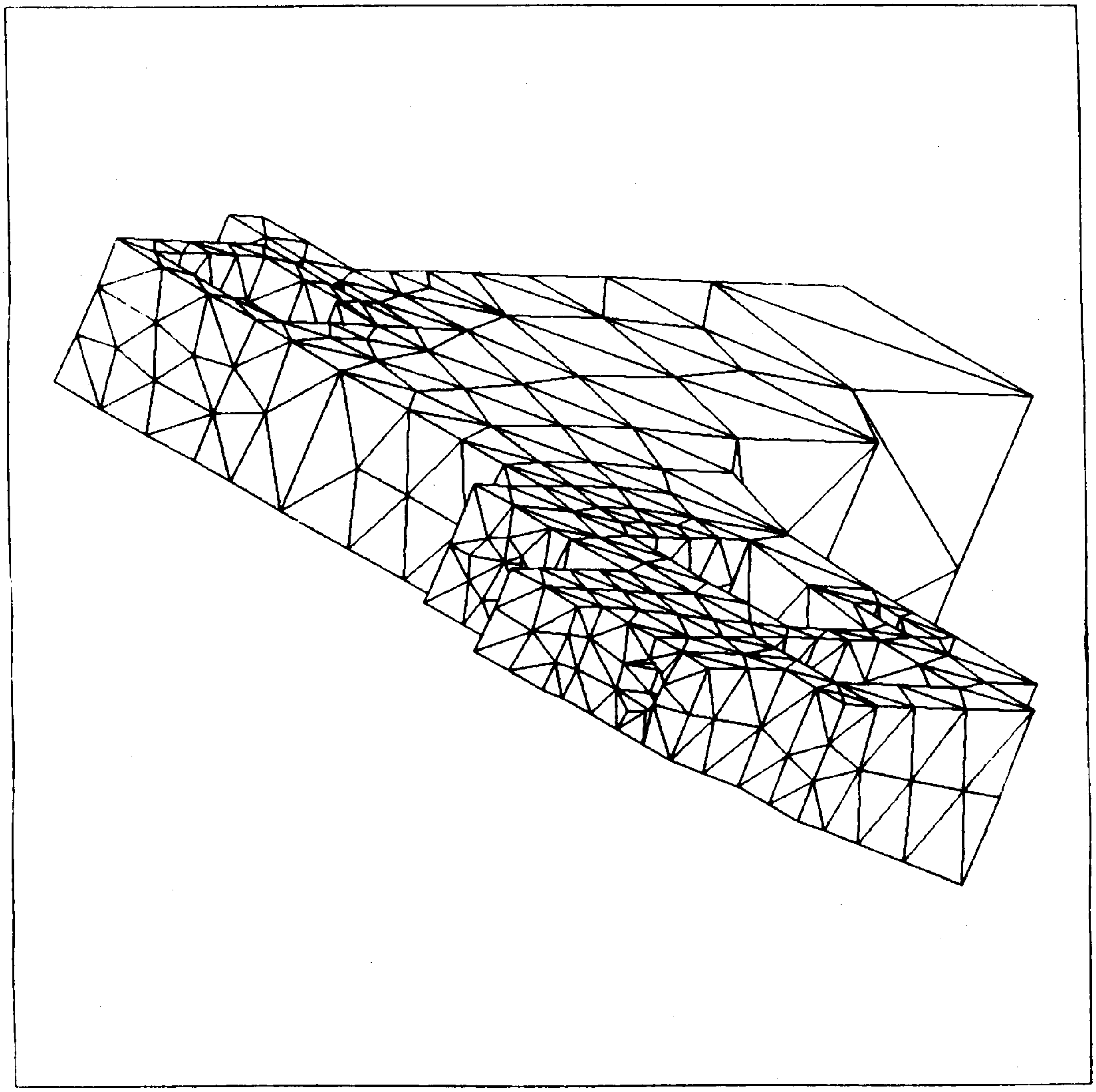

Fig. A-14 Hidden Line Plot of Detailed HPOTP Main Pump Housing Sector Model from 320 to 332°

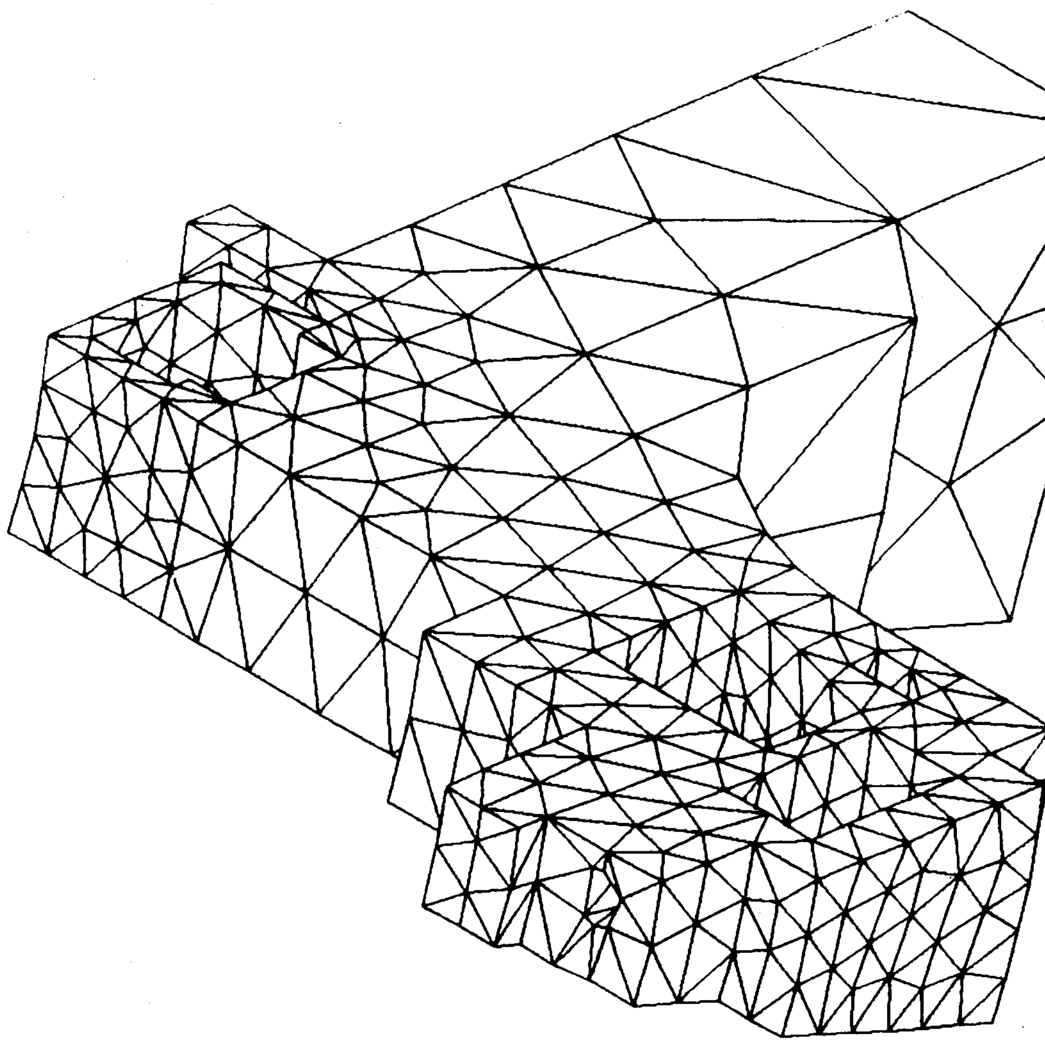

Fig. A-15 Hidden Line Plot of Detailed HPOTP Main Pump Housing Sector Model from 336 to 352°

Table A-2 DIRECTORY OF FILES ON MAGNETIC TAPE

File Name	File Type*
S0E12	14
S16E38	14
S40E52	14
S60E72	14
S80E98	14
S100E112	14
S116E176	14
S180E192	14
S200E212	14
S220E232	14
S238E254	14
S256E268	14
S270E312	14
S320E332	14
S336E352	14
S0N12	15
S16N38	15
S40N52	15
S60N72	15
S80N98	15
S100N112	15
S116N176	15
S180N192	15
S200N212	15
S220N232	15
S238N254	15
S256N268	15
S270N312	15
S320N332	15
S336N352	15

*'14' denotes ANSIS FILE14 (elelment listing).
'15' denotes ANSIS FILE15 (node listing).